NMR CHARACTERIZATION OF PARATHION: PROPERTIES, TRANSPORT, AND REACTION KINETICS

by

Emma Catherine Baker

A thesis

submitted in partial fulfillment

of the requirements for the degree of

Master of Science in Chemistry

Boise State University

May 2012

BOISE STATE UNIVERSITY GRADUATE COLLEGE

DEFENSE COMMITTEE AND FINAL READING APPROVALS

of the thesis submitted by

Emma Catherine Baker

Thesis Title: NMR Characterization of Parathion: Properties, Transport, and Reaction Kinetics

Date of Final Oral Examination: 14 March 2012

The following individuals read and discussed the thesis submitted by student Emma Catherine Baker, and they evaluated her presentation and response to questions during the final oral examination. They found that the student passed the final oral examination.

Owen McDougal, Ph.D.	Chair, Supervisory Committee
Gerry Chingas, Ph.D.	Member, Supervisory Committee
Dale Russell, Ph.D.	Member, Supervisory Committee

The final reading approval of the thesis was granted by Owen McDougal, Ph.D., Chair of the Supervisory Committee. The thesis was approved for the Graduate College by John R. Pelton, Ph.D., Dean of the Graduate College.

ACKNOWLEDGEMENTS

There are several people that have been instrumental in putting together the work presented in this thesis. My thesis committee- Dr. Owen McDougal, Dr. Gerry Chingas, and Dr. Dale Russell- deserve acknowledgements for their direction and support. Emily Drussel is recognized for the biphasic NMR studies. Others instrumental to early investigations include Taylor Dixon, Ben Parker, Bryan Martin, and Mark Swartz. This work was supported by funding from Boise Technology, Inc., Department of Defense: Defense Threat Reduction Agency grant W81XWH-07-1-0004, and the National Science Foundation CRIF-MU/RUI (0639251).

ABSTRACT

The hydrolysis reaction of parathion (PTH) to produce *para*-nitrophenolate (pNP) and O,O-diethylthiophosphate (DETP) was examined in a minimally disturbed liquid-liquid biphasic reaction system by proton and phosphorous nuclear magnetic resonance spectroscopy. The effect of the micellar cationic surfactant, cetyltrimethylammonium chloride (CTAC), on PTH transport, hydrolysis, and system characteristics including reactant-product concentrations, pNP partition coefficients, pNP surface activity, ultraviolet degradation of pNP, oxidation of pNP, and impurities in PTH are reported. Surfactant reaction systems resulted in a 2.5 order of magnitude increase in the amount of PTH transported into the aqueous layer as compared to the control system at 2100 h. A comparison between the total concentration of reaction products, pNP and DETP, in the control system without surfactant and in the presence of 33.3 mM CTAC varied by less than 5%. Interestingly, the total amount of pNP detected in the bulk organic and aqueous layers was five to six times lower than DETP, independent of surfactant. This apparent discrepancy in the concentration of pNP was investigated and was concluded to arise from an impurity present in the ampules of PTH. This impurity was disguised because the chemical shifts of DETP and PTH overlapped in deuterated chloroform. The impurities were revealed when the PTH was dissolved in deuterated benzene. The kinetics of the reaction between PTH and NaOD in absence of surfactant were also determined by running single phase experiments that were mixed before analysis at 0 mM NaOD, 5.33 mM NaOD, 33.33 mM NaOD, and 100 mM NaOD. An experiment at

100 mM DCl was also conducted to ensure that there was no acid hydrolysis occurring at room temperature. There was no reaction occurring at the 100 mM DCl or the 0 mM NaOD. The pseudo-first order rate for the 5.3 mM NaOD system was determined to be $1.9 \times 10^{-4} (\pm 4 \times 10^{-5})$ min^{-1}. The 33.3 mM NaOD pseudo-first order rate was determined to be $1.4 \times 10^{-3} (\pm 2 \times 10^{-4})$ min^{-1}. The pseudo-first order rate for the 100 mM NaOD was determined to be $3.8 \times 10^{-3} (\pm 4 \times 10^{-4})$ min^{-1}. When the pseudo-first order rate was plotted versus OD^- concentration, the second order rate constant was determined to be $3.90 \times 10^{-5} (\pm 8 \times 10^{-7})$ $mM^{-1}min^{-1}$. The conclusion of this work is that CTAC facilitates transport of PTH, changes product solubility characteristics, and does not significantly enhance degradation of organophosphates. The reaction between PTH and NaOD in the absence of surfactant increased linearly, as expected, with respect to OD^- concentration.

TABLE OF CONTENTS

LIST OF TABLES

LIST OF FIGURES

LIST OF SCHEMES

LIST OF EQUATIONS

LIST OF ABBREVIATIONS

BSU	Boise State University
$CDCl_3$	Chloroform-D
C_6D_6	Deuterated Benzene
cmc	Critical Micelle Concentration
CTAC	Cetyltrimethylammonium Chloride
CWA	Chemical Warfare Agent
D_2O	Deuterium Oxide
DETP	O,O-diethylthiophosphate
DSS	Sodium 2,2-dimethyl-2-silapentane-5-sulfonate
GA	Tabun
GB	Sarin
GC	Gas Chromatography
GC-MS	Gas Chromatography- Mass Spectrometry
GD	Soman
GF	Cyclosarin
HCN	Hydrogen cyanide

MEPTH	Monoethylparathion
MSDS	Material Safety Data Sheet
NaOD	Sodium Deuteroxide
NMR	Nuclear Magnetic Resonance
OP	Organophosphate
$P_{o/w}$	Partition Coefficient of a species between oil and water
pNP	*para*-Nitrophenolate
PTH	Parathion
TDC	Thesis and Dissertation Coordinator
TMS	Tetramethylsilane
U.S.	United States
UV	Ultraviolet
UV-VIS	Ultraviolet Visible Spectroscopy
WWI	World War I
WWII	World War II

BACKGROUND AND INTRODUCTION

Chemical Warfare Agents

Chemical warfare agents (CWAs) have been used throughout history. Their first recorded use was in the form of toxic smokes used by the Egyptians, Babylonians, Indians, and Chinese as early as 3000 B.C.E. In the modern age, John Doughty suggested the United States use chlorine gas as a CWA during the Civil War; the idea was rejected.[1] The gas was first used as a CWA by the Germans in World War I (WWI). Of the estimated 3000 chemical substances considered for development into warfare agents in WWI, several new CWAs were developed including phosgene, diphosgene, and mustard gas. During WWI, from 1914 until 1918, approximately one million of the 26 million total casualties were due to CWAs.[2] During this same era, the use of these gases as insecticides was investigated. Hydrocyanic acid (HCN) was used to control pests in mills and storehouses, and it was also used by the military to delouse uniforms and equipment. HCN was not used as a CWA until WWII, when it was used by the Nazis to exterminate the Jews in concentration camp gas chambers.[3]

Organophosphates (OP's) were among the first CWAs classified as nerve agents. Tetraethyl pyrophosphate was the first OP synthesized in 1854. It was not until the 1930s that the devastating effects of OP's were discovered, when the German chemist Willy Lange was accidentally exposed and noticed strange effects.[1] OP's are carbon-containing derivatives of phosphoric acid that affect the nervous system by inhibiting acetylcholinesterase. In a normally functioning brain, neurons communicate by

producing a chemical signal caused by acetylcholine binding to acetylcholine receptors. When the communication is completed, acetylcholinesterase ends signal transmission by converting acetylcholine into acetate and choline. When the OP's are introduced, they bind to the acetylcholinesterase, which then can no longer degrade the acetylcholine to end signal transmission. This continuous signal transmission, called a *cholinergic crisis*, causes nausea, blurred vision, diarrhea, headaches, seizures, paralysis, and possibly death. [1, 4, 5]

Organophosphates were initially studied for use as insecticides; however, their effectiveness as CWAs was discovered and exploited during World War II, circa 1942. Tabun (GA) was the first OP used as a CWA in 1936, followed by sarin (GB) in 1938. Other OP agents created around this time were soman (GD) and cyclosarin (GF). Another OP nerve agent, VX, was developed in 1952. During WWII, Germany made 78,000 tons of OP's, including 12,000 tons of tabun and 0.5 tons of sarin. At a toxicity of 100-200 mg min/m^3, the 12,000 tons of tabun alone that Germany produced was enough to kill 60 billion people. [1]

In 1969 the United States stopped production of OP CWAs, and in 1975 President Ford signed the Geneva Protocol, which prohibited use of CWAs.[1] Although the U.S. does not use OP's as CWAs, there is still the risk of exposure to U.S. soldiers and civilians in other parts of the world. The 1995 incident, when a terrorist group released sarin gas in the Tokyo subways, is a well-known example. Thirteen people were killed, fifty were severely injured, and over 1,000 people were affected with vision problems and other mild symptoms.[6]

The agricultural community still uses OP's as pesticides. These OP's are typically much less toxic than the CWA OP's, although they still inhibit acetylcholinesterase and can still induce a cholinergic crisis with sufficient exposure. Parathion is one organophosphate pesticide that was in use in the United States (U.S.) until the EPA banned it in 1991 due to health risks.[7,8] There are still many OP pesticides permitted by the EPA for use in the U.S., including dichlorvos, malathion, and tribufos.[9]

The discovery of nerve agents in WWII prompted scientists to develop decontamination methods for OP's. One of the first decontamination methods was a super-chlorinated bleach solution. This was commonly used in WWII and is still used to a lesser extent today, when a dedicated decontamination kit is unavailable. There are several problems associated with the use of super-chlorinated bleach to decontaminate OP's, including corrosiveness to surfaces, the ineffectiveness of chlorine over time, and the large volumes needed for complete decontamination. [4]

Current decontamination kits consist of a solution composed of 70% diethylenetriamine, 28% ethylene glycol monomethyl ether, and 2% sodium hydroxide solution. This formulation is stable for long periods of times and is not corrosive to metal; however, it is still damaging to paints, plastics and rubber material and has also been shown to have some degree of teratogenicity in rats. [2,4] Due to these unfavorable effects, a different method for decontamination would be beneficial.

For research into decontamination methods, several OP pesticides that also act as acetocholinesterase inhibitors can be used to simulate more dangerous OP CWAs. Parathion (PTH) serves in this capacity as an accepted VX proxy for the development of

decontamination protocols because of its lower toxicity. In rats, the oral ingestion LC_{50} is 2 mg/kg for PTH and 0.08 mg/kg for VX. [10,11]

The mechanism for OP decontamination typically occurs by hydrolysis at the phosphorus, since most OP's react with water. However, OP's are typically nonpolar oils with limited or no solubility in water; the solubility of PTH is 24 ppm by volume at 25°C.[12] Consequently, hydrolysis of OP's is very slow, the half-life of PTH being 2600 h at pH 7.4 and 25°C. [13] Attempts to increase the hydrolysis rate required for the degradation of OP's include use of enzymes,[4,14] use of metal ions,[4,14,15] and reaction acceleration by micelles or emulsions.[4,15-21] The present work began with exploring the use of micellar surfactants to enhance reactivity of the OP PTH. We hypothesized that surfactants might transport PTH into water and thus increase the rate of hydrolysis.

Surfactants

The surfactant used in this study is CTAC, illustrated in Scheme 1.1. It is a typical surfactant in that it is composed of a hydrophilic head group and a hydrophobic tail. The head group favors polar solvents like water, while the hydrophobic tail prefers a non-polar solvent. Because surfactants have functional groups with a propensity for both polar and non-polar solvents, it is not energetically favorable for the surfactant to exist in either a purely polar or non-polar environment.[22]

Scheme 1.1. Structure of the surfactant, cetyltrimethylammonium chloride (CTAC), identifying the hydrophilic and hydrophobic regions of the molecule.

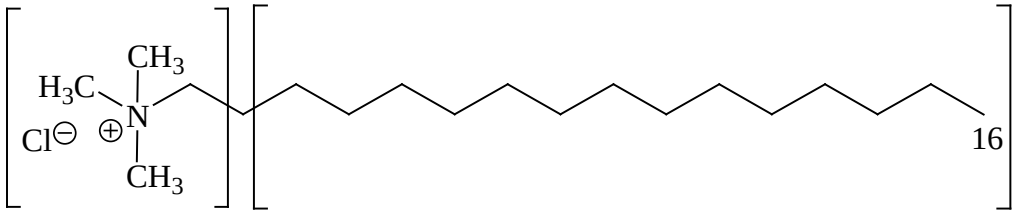

Hydrophilic Head Hydrophobic Tail

Therefore, in an aqueous/oil biphasic system, and at low concentrations, the surfactant will concentrate at the interface between polar and nonpolar components.[22] This tendency causes surfactants to increase the degree of association of the nonpolar layer with the polar layer [22,23]

At higher surfacteant concentrations, starting with the critical micelle concentration (cmc), it becomes energetically favorable for surfactants to aggregate into micelles. Micelles form so that either the hydrophilic head or hydrophobic tail is protected from either the non-polar or polar solvent, respectively.[23] For instance, if the solvent is water, a very polar liquid, the micelle will form with the polar heads oriented toward the water and the hydrophobic tails tucked inside the micelle core where they have no contact with water. CTAC micelles are typically composed of 30-200 surfactant molecules. The shape of the micelle can vary widely, from ellipsoid, spherical, disk-shaped, to rod-shaped.[22] In a biphasic system, a micelle can act as a transfer agent, by encapsulating components from the non-polar oil layer into its non-polar core, and then migrating into the polar layer, as facilitated by the micelle's polar surface.[22-24]

NMR CHARACTERIZATION OF PARATHION INTERFACIAL TRANSPORT AND HYDROLYSIS IN AN UNDISTURBED BIPHASIC SYSTEM

Introduction

The transport across the boundary of biphasic OP-water interfaces is significant to the development of effective chemical and biological decontamination formulations. The mechanism of PTH hydrolysis in solution has been studied extensively, but these studies use vigorous mixing of oil and/or water to accelerate hydrolysis.[4,7,10,14,17-20,25] In contrast, we report the first characterization of PTH hydrolysis in a minimally disturbed liquid biphasic reaction medium, i.e. subjected only to diffusive and slow convective transport, in the presence and absence of a cationic surfactant by NMR spectroscopy.

Hydrolysis of PTH occurs by nucleophilic attack of the thiophosphate bonds of PTH, resulting in the production of either *para*-nitrophenolate (pNP) and O,O-diethylthiophosphate (DETP) or monoethyl parathion (MEPTH) and ethoxide(Scheme 2.1a).[14-17,20] Alkaline conditions, with higher concentrations of nucleophilic hydroxyl ions, facilitate the reactions. In this study, CTAC was also added to facilitate PTH transport into the aqueous layer where hydrolysis occurs. Both pathways were observed, dependent on conditions (Scheme 2.1a). At high pH and low CTAC concentrations, the primary pathway dominated as evidenced by sole detection of the reaction products pNP and DETP. On the other hand, MEPTH was detected at higher concentrations of CTAC.

Addition of CTAC not only increased micellar concentration but lowered solution pH as well.

Cationic surfactants are known to form micelles which can complex to nucleophiles at and above their critical micelle concentrations (cmcs).[7,10,14-17,19-21,25-27] We found that high concentrations of CTAC increased the amount of PTH transported into the aqueous layer, thus confirming the model of micellar encapsulation of PTH. A model for the biphasic reaction system, based on reactant and product monitoring, trends in pH, product partition coefficients, and literature information is shown Scheme 2.1b.[22-24]

Scheme 2.1. The hydrolysis reaction of PTH by S_N2 nucleophilic attack showing (a) primary and alternate reaction mechanisms for PTH hydrolysis and (b) a cartoon representation of the biphasic reaction system, an NMR tube with CTAC concentration well above the cmc.

(a)

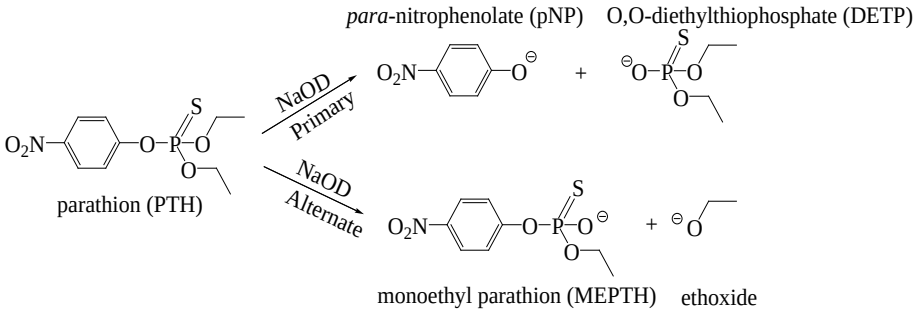

(b)

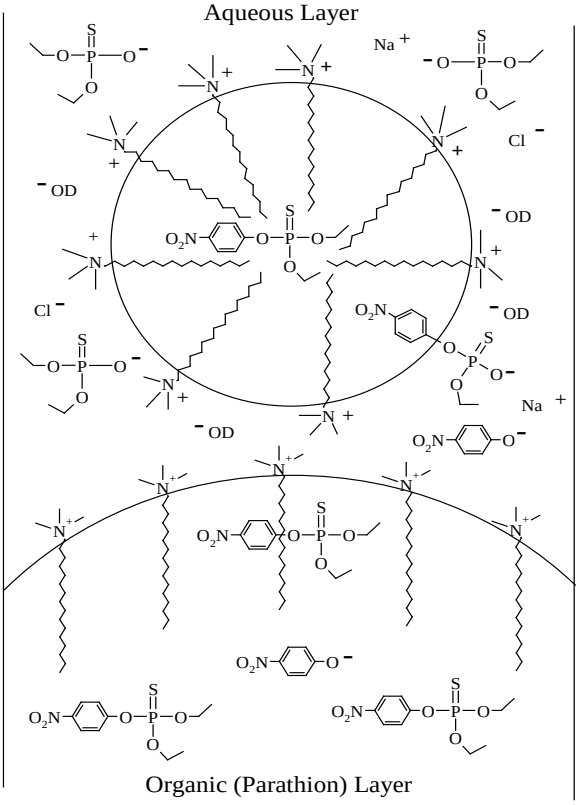

The unanticipated complexity of experimental results, however, prevented unambiguous confirmation of this model. The most perplexing of these was the consistent discrepancy between the expected and observed stoichiometry of the reaction products. Specifically, the amount of pNP was lower as compared to DETP. Four hypotheses were initially tested: (a) that the pNP migrated into the organic PTH layer as determined by its partition coefficient between the aqueous and PTH phases; (b) pNP is surface active;[28-31] (c) pNP is degrading because of UV exposure;[32] (d) pNP is reacting to form by-products undetectable by NMR.[33]

The first explored explanation for the discrepancy is that the missing pNP was present in the oil layer, which was kept below the NMR receiver coil to avoid PTH layer detection. Measurement of partition coefficients for pNP showed that, while pNP was present in the PTH layer, it was not present in enough quantity to account for the stoichiometric discrepancy.

The second possibility, presented in the literature, suggests that pNP congregates at the PTH surface in biphasic systems. This behavior has been attributed to favorable π-π stacking interactions between pNP and PTH in combination with solvophobic forces between pNP and the polar aqueous layer.[28-31] In a surface activity experiment, pNP was not observed in sufficient quantities at the surface to account for the stoichiometric inequivalence.

The third hypothesis, another literature precedent, is that pNP might form free radicals upon exposure to UV light that degrade into products undetectable by NMR.[32] However, upon exposure to UV light, our system showed no significant degradation of pNP.

The fourth explanation for the lower amount of pNP as compared to DETP is that pNP is reacting by an unanticipated mechanism to form byproducts that are unobservable by NMR.[33] Several single phase experiments, consisting of the aqueous phase at various hydrolyzing strengths, were set up to determine if pNP concentration was changing; it was not. However, these experiments did reveal that there was more initial DETP present than expected. This impurity was undetected during initial sample screening because, in deuterated chloroform solvent, both of the aliphatic resonances of DETP overlapped with the aliphatic resonances of PTH. When D6 benzene was used for the sample screening by ^{1}H NMR the impurity was revealed.

Experiments conducted throughout this study can be grouped into two categories: 1) long-term NMR analysis of the aqueous phase of the minimally disturbed biphasic reaction systems to characterize components; and 2) investigation of the stoichiometric discrepancy, further subdivided into: (a) determination of the partition coefficient for pNP between the aqueous and organic phases for each reaction system; (b) pNP surface activity in a control biphasic reaction system; (c) UV degradation study of pNP; and (d) pNP aqueous environment reaction study.

Materials

Neat ethyl parathion was purchased from Supelco (49062). PTH is a hazardous chemical that requires adherence to appropriate handling protocol per the MSDS. Cetyltrimethylammonium chloride (99% purity) was purchased from Acros Organics (411410050). Sodium deuteroxide (NaOD) was purchased from Cambridge Isotope Laboratories, Inc. with 40% (w/w) in D_2O (DLM-45-50). Deuterium oxide (D_2O) was purchased from Cambridge Isotope Laboratories, Inc. (DLM-4-99-100). *para*-

Nitrophenol was purchased from Sigma-Aldrich at ≥ 99% purity (241326-50G). O,O-Diethylthiophosphate potassium salt was purchased from Sigma Aldrich at ≥ 98% purity (445177-5G). Chloroform-D ($CDCl_3$) (1% (v/v) TMS) ≥ 99.8% purity was purchased from Acros Organics (A0242754). Deuterated benzene (C6D6) was purchased from Cambridge Isotope Laboratories, Inc. (DLM-1-25). DCl was purchased from Acros Organics. Sodium 2,2-dimethyl-2-silapentane-5-sulfonate (DSS) was purchased from Cambridge Isotope Laboratories, Inc. (DLM-32-1). NMR tubes of 5 mm (OD) x 9 in. were purchased from Bruker BioSpin (Z107374).

Methods

All NMR data were acquired at 20ºC on a Bruker AVANCE III 600 MHz spectrometer equipped with a 5 mm TXI probe for ^{1}H NMR spectra and a BBO probe for ^{31}P NMR. The zg30 pulse sequence with a 1 sec d1 delay was used for ^{1}H NMR spectra, and a proton decoupled phosphorous zgpg30 with a 2 sec d1 delay was used for ^{31}P NMR spectra, both from the Bruker sequence library. Samples were stored at room temperature and were run at 20^{o}C in the probe. All experiments were scaled according to receiver gain and number of scans to allow for direct comparison of concentrations. All samples were run in 5mm NMR tubes.

Biphasic Aqueous Component Characterization

For long-term studies of PTH hydrolysis, biphasic reaction systems were prepared by placing an oil layer (75 µL PTH) at the bottom of the NMR tube with a 12 in. needle and syringe and then carefully pipetting the aqueous solution (475 µL), pH of 11.9, over the top of the PTH layer, taking care to minimize interfacial mixing. The total volume of

the system was 550 μL. The meniscus was placed below the receiver coil of the NMR probe to minimize signal from the oil layer. Table 2.1 shows the composition of components in the control reaction without surfactant and the reaction conditions with CTAC concentrations below, at, and above the cmc. The aqueous phase of each reaction was minimally disturbed, in the sense that there was no shaking or vortexing of the reaction mixture during preparation. However, slight mixing may have occurred due to transportation and room temperature variation during storage. The sample was immediately monitored by ^{1}H NMR spectroscopy; 1024 scans were taken for each spectrum. Peak integration using the Bruker macros, intser/'global integration', was used to quantitate PTH, pNP, DETP, and MEPTH by comparing to a DSS standard.

Table 2.1. Sample component composition for each biphasic reaction. The oil layer (PTH) in each system was 75 μL and the aqueous layer (salt, surfactant, and deuteroxide when applicable) was 475 μL.

Reaction Conditions	PTH (μL)	NaOD (mM)	NaCl (mM)	Surfactant (mM)
Control	75	33.3	33.3	-
CTAC	75	33.3	33.0	0.33
CTAC	75	33.3	30.0	3.33
CTAC	75	33.3	23.3	10.0
CTAC	75	33.3	15.0	18.0
CTAC	75	33.3	-	33.3

Immediately following preparation, the first 20 h of the aqueous phase of the reaction was monitored by a series of hour-long (1024-scans) NMR acquisitions. Follow-

up acquisitions were run at more widely-spaced times, up to 2100 h after initial acquisition.

A typical spectrum containing CTAC is shown in Figure 2.1, while a spectrum without CTAC is shown in Figure 2.2. To avoid confusion due to minor variations in chemical shifts, molecular identities of the protons responsible for the spectral lines are assigned by letter in Scheme 2.2. Their positions in the ^{1}H spectrum are identified by letter in Figures 2.1 and 2.2. Variations in their chemical shifts in different solvents are tabulated in Table 2.2.

Representative ^{1}H NMR spectra are shown for the system under all reaction conditions after 2100 h (Appendix A.1). Differentiation between PTH and MEPTH, and assignment of the latter, was confirmed by comparison of the relative ratio of protons in the aromatic region to the corresponding aliphatic resonances between 3.5 to 4.0 ppm.

Proton spectra were analyzed for the aromatic ring protons of PTH (A1 and A2), the aromatic ring protons of MEPTH (B1 and B2), the aromatic ring protons of pNP (C1 and C2), the aliphatic protons of PTH (A3 and A4), the aliphatic protons of MEPTH (B3 and B4) and the aliphatic proton resonances of DETP (D1 and D2). Although the upfield MEPTH and PTH doublets overlap at 7.3 ppm in D_2O, the downfield aromatic resonances for MEPTH and PTH near 8.1 ppm are resolvable ($\Delta\delta \geq 30$ Hz), as are the aliphatic protons around 4.0 ppm. No aliphatic protons were observable around 1.1 ppm due to overlap with CTAC resonances.

Scheme 2.2. Designation of protons in a. PTH; b. MEPTH; c. pNP; and d. DETP

a.

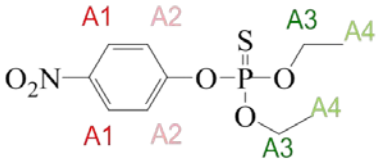

b.

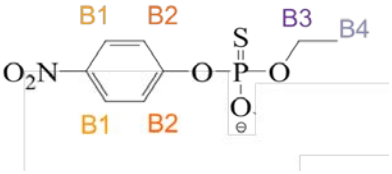

c

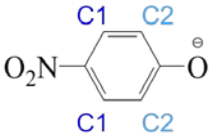

d.

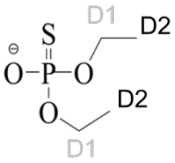

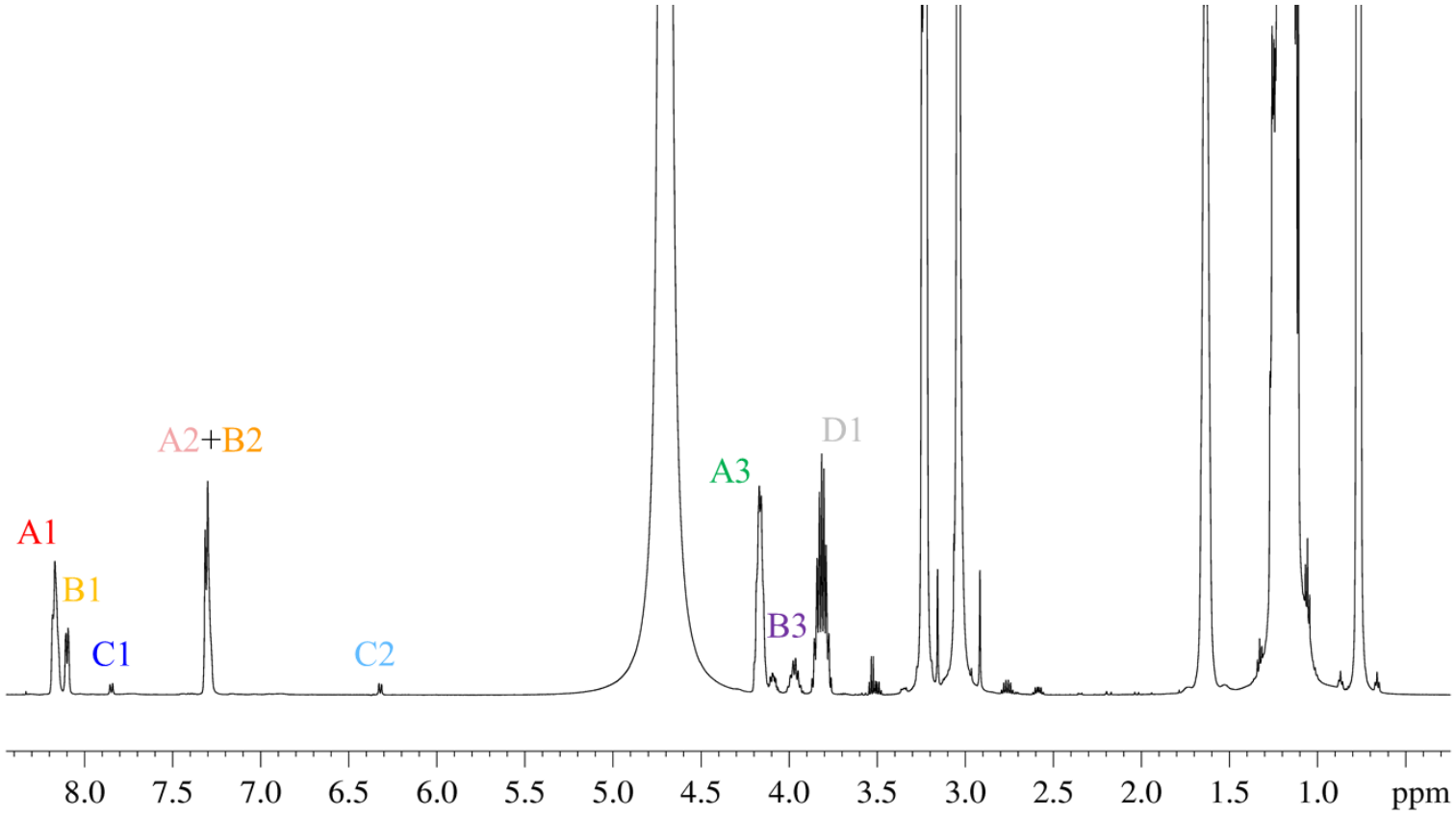

Figure 2.1. Full spectrum of biphasic reaction system where the aqueous (top) phase was prepared using D2O, 33.33 mM CTAC, and 33.33 mM NaOD, and the oil (bottom) phase was 75 uL of PTH. The spectrum has labels for PTH (A series), MEPTH (B series), pNP (C series), and DETP (D series). No resonances could be isolated for A4, B4, and D2 due to overlap with CTAC proton resonances.

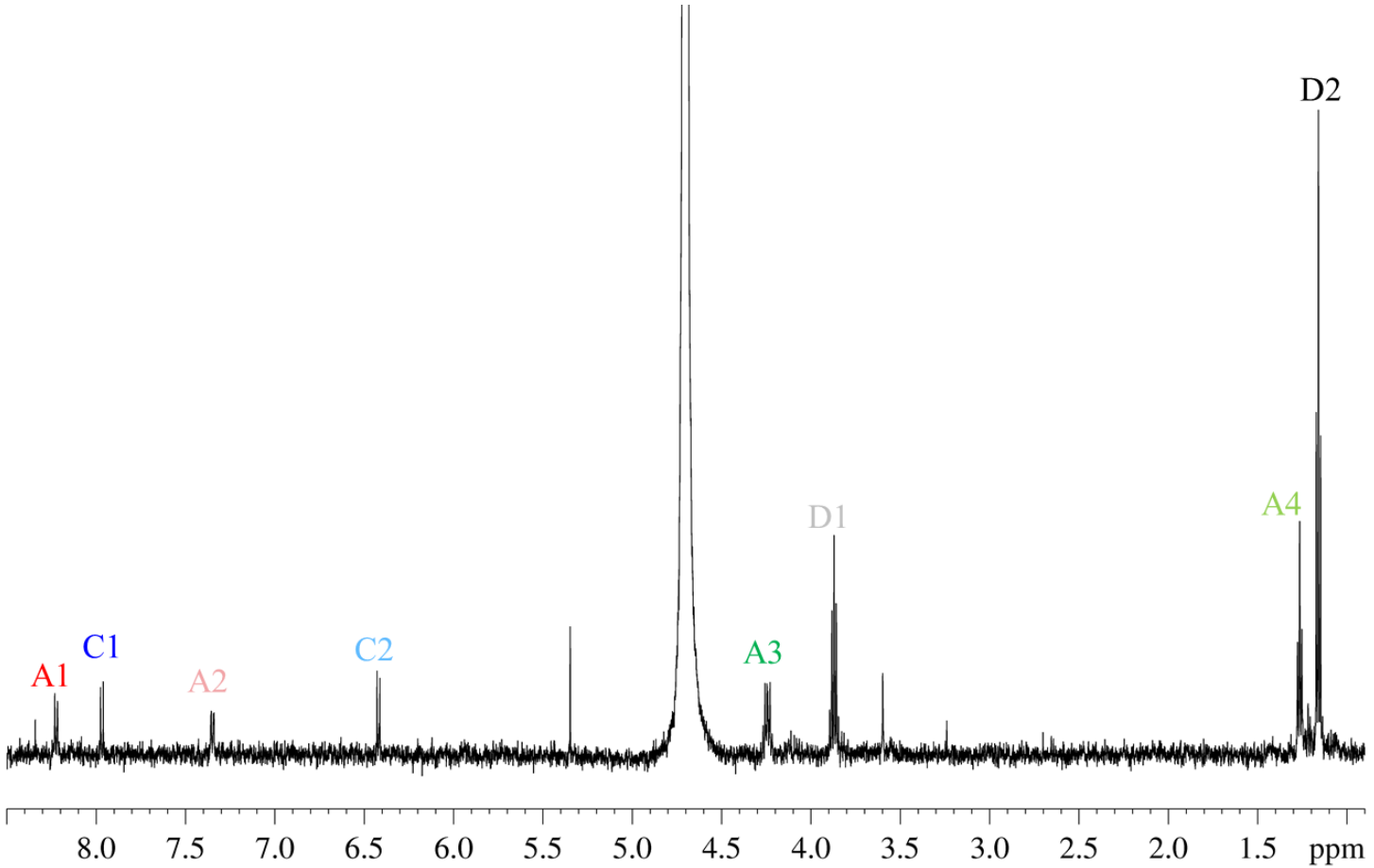

Figure 2.2. Full spectrum of single phase reaction system consisting of D2O, 5.3 mM NaOD, 194.7 mM NaCl, and dissolved PTH with PTH(A series), pNP (C series), and DETP (D series) labels

Table 2.2. Chemical shift values in ppm of protons of PTH (A series), MEPTH (B series), pNP (C series), and DETP (D series) while in D_2O, $CDCl_3$ and D6 Benzene. Chemical designations are provided by Scheme 2.2.

	PPM		
Designation	**D2O**	**CDCl3**	**D6 Benzene**
A1	**8.21**	**8.27**	**7.70**
A2	**7.30**	**7.36**	**6.90**
A3	**4.23**	**4.29**	**ND**
A4	**1.25**	**1.41**	**0.96**
B1	**8.10**	**ND**	**ND**
B2	**7.31**	**ND**	**ND**
B3	**3.97**	**ND**	**ND**
B4	**ND**	**ND**	**ND**
C1	**7.95**	**ND**	**7.90**
C2	**6.40**	**ND**	**6.29**
D1	**3.86**	**ND**	**ND**
D2	**1.15**	**ND**	**0.88**

Investigations into Stoichiometric Discrepancy

Partition coefficient determination. Following the 2100 h NMR examinations, partition coefficients for pNP and DETP were determined for each set of reaction conditions listed in Table 2.1. An 11 in. glass pipette was used to extract an aliquot of the aqueous phase, which was placed in a 2 mL Eppendorf tube. 250 µL was extracted using an automatic pipette and mixed with 5.8 mg DSS. This aqueous solution was combined

with 350 μL D_2O, also measured by automatic pipette, and transferred to a 5 mm NMR tube for observation. For the oil phase, approximately 20 μL of the oil layer was transferred with a glass syringe from the biphasic reaction tube into an NMR tube to which 555 μL of $CDCl_3$ (1% (v/v) TMS) was added. To determine pNP concentrations ^1H NMR spectra were acquired for both the aqueous and organic samples using 512 scan acquisitions. The amount of pNP was determined by comparison with TMS and DSS concentrations present in the oil and aqueous phases, using peak integration to compare line intensities. The starting concentration of pNP in each of the phases could then be determined by back-calculation. The partition coefficient for pNP in each reaction system was finally calculated using Equation 1:[34]

$$P_{O/W} = [pNP]_O / [pNP]_W \qquad \text{Eq. 2.1}$$

where and $P_{O/W}$ is the partition coefficient of pNP in the biphasic reaction system, $[pNP]_O$ is the concentration of pNP present in the PTH layer, and $[pNP]_W$ is the concentration of pNP present in the aqueous layer. To avoid error from overlapping spectral lines, we attempted to use ^{31}P NMR to determine DETP concentrations similarly. However, the absence of the DETP resonance at 54.9 ppm in the ^{31}P NMR spectra of the oil phase sample indicated that DETP was present solely in the aqueous layer. The DETP partition coefficient was therefore set to zero.

Monitoring of pNP surface activity in a mimic control biphasic reaction. A sample was prepared to test the surface activity of pNP. An aqueous solution was prepared to replicate conditions found in the control reaction sample *circa* 2100 h. In a 5mm NMR tube, 9.37 mM DETP potassium salt and 12.24 mM *p*NP was dissolved in 475 μL of D_2O/NaOD solution with a pH of 11.8. A ^1H NMR reference spectrum was

acquired. Next, 75 µL of PTH was carefully introduced into the bottom of the NMR tube, pushing the aqueous phase up as PTH was added. The result was a biphasic mimic system that already contained a known amount of pNP and DETP in the aqueous layer. The mimic system was monitored every hour for 15 h and then again after one week and after two weeks. After two weeks, a glass pipette was used to gently agitate the interfacial region of the biphasic system by flushing with the aqueous layer across the surface of the meniscus. The agitated sample was monitored immediately, after one day, and again after 18 days by ^{1}H NMR spectroscopy. In parallel, a control biphasic reaction tube that had reacted for 2100 h was also flushed at the interface by pipette. Monitoring by ^{1}H NMR occurred after one week and again after two weeks.

Monitoring ultraviolet degradation of pNP**.** To test the possibility of photodegradation of pNP, two NMR samples were prepared, similar to the reaction control model discussed above, but here without PTH. Each contained 550 µL of D_2O solution with 18.75 mM NaOD, 12.25 mM pNP, 9.38 mM DETP potassium salt, and 12.5 mM NaCl. One tube was wrapped in aluminum foil while the other tube was exposed to daylight. After four weeks of exposure to ultraviolet (UV) light from the sun, the levels of pNP were monitored and compared to DETP levels.

Monitoring for additional reactions of pNP**.** In order to check for pNP degradation due to mechanisms such as oxidation, we decided to monitor a single phase reaction with no surfactant present. To do this, surfactant-free aqueous phases were prepared with different concentrations of NaOD: 0 mM, 5.3 mM, 33.3 mM, and 100 mM. NaCl was added to maintain ionicity in accordance with Table 2.3. A 2700 µL aliquot of aqueous phase was added to a 15 mL falcon tube, which was then cooled to 10^{o}C. The

purpose of cooling to 10^{o}C was to eliminate the possibility of PTH condensation while working near room temperature. After cooling, 60 µL PTH were added to the falcon tube, which was then vortexed for 30 seconds. This unsaturated aqueous-PTH mixture was then centrifuged for 5 minutes at 2600 RPM using a Centra-CL2 centrifuge with 15 mL falcon tube inserts. The aqueous phase (600 µL) was carefully pipetted to separate it from the PTH oil. The aqueous extract was directly transferred to an NMR tube for analysis at 20^{o}C. Three NMR tubes were prepared in this manner. One tube was immediately monitored by ^{1}H NMR spectroscopy; 256 scans were taken for each spectrum over a 17 h period. The other tubes were monitored after 24 h to ensure that product and reactant concentrations behaved consistently. Areas of relevant peaks were capered to determine concentrations.

Table 2.3. Composition of single-phase reaction samples. The oil (PTH) in each system was 60 μL and the aqueous volume containing salt, deuterium oxide, and NaOD when applicable, was 2700 μL.

Reaction Conditions	PTH (μL)	NaOD (mM)	NaCl (mM)
Control	60	0	200
Hydrolyzing	60	5.3	194.7
Hydrolyzing	60	33.3	167.7
Hydrolyzing	60	100	100

The aqueous phase of the reaction was monitored by NMR every fifteen minutes for 16 h. Areas of proton lineshapes were analyzed for the aromatic ring protons of PTH: A1 and A2; the aromatic ring protons of pNP: C1 and C2; the aliphatic protons of PTH: A3 and A4; and the aliphatic proton resonances of DETP: D1 and D2. Intensities of some resonances are unreported because they were compromised by overlap.

Results

Biphasic Aqueous Component Characterization

An increase in PTH and PTH hydrolysis reaction products (pNP, DETP, and MEPTH) was observed with increasing CTAC concentrations (Figure 2.1). For CTAC concentrations ranging from 0.333 mM to 33.3 mM, after 2100 h of reaction, aqueous concentrations of PTH increased from 0.15 mM to 23.6 mM, pNP increased from 0.04 mM to 1.0 mM, DETP increased from 16.8 mM to 27.1 mM, and MEPTH increased from 0.13 mM to 7.95 mM, respectively. For the control reaction in the absence of CTAC, the aqueous phase concentrations of PTH, pNP, DETP, and MEPTH were 0.05 mM, 3.56

mM, 26.3 mM, and 0.10 mM respectively. These data indicate that significantly higher amounts of DETP are present as compared to pNP. In addition, the concentration of PTH in the aqueous phase was observed to increase with surfactant concentration. A finding that persisted during the course of these studies was that the levels of DETP in the system were not stoichiometrically equivalent with the levels of pNP, i.e., either pNP should be present in larger amounts, or DETP should be present in smaller amounts.

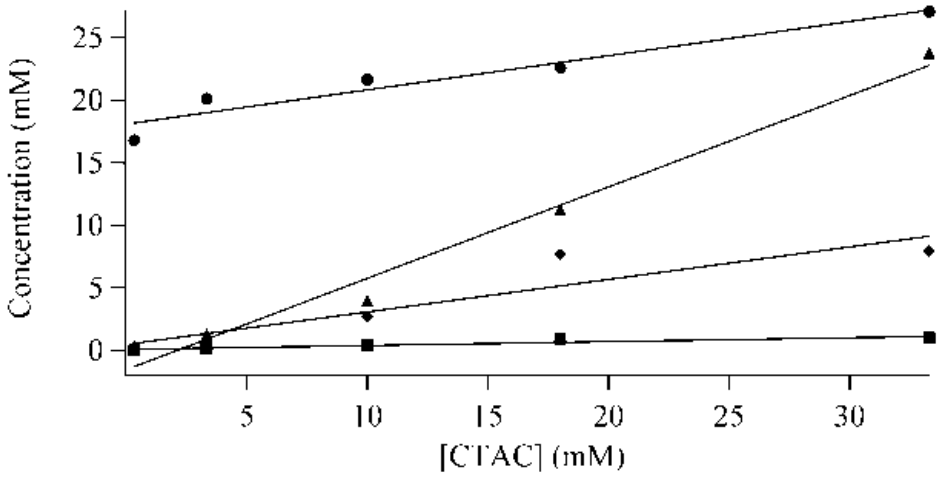

Figure 2.3. Concentration of PTH and products in the aqueous layer (▲ PTH; ■ pNP; ● DETP; ♦ MEPTH) at CTAC concentrations from 0.333 to 33.3 mM after a 2100 h reaction time. The control system is not shown here but produced 0.05 mM PTH, 3.56 mM pNP, 26.3 mM DETP, and MEPTH 0.10 mM. The proton resonances plotted here are A1, B1, C2, and D1

The appearance of increasing amounts of PTH in the aqueous layer is consistent with CTAC being surface active in lower concentrations, followed by micelle facilitated transport at higher concentrations.[4,15-21] Figure 2.2 shows a stack plot of the ^{1}H NMR spectra for aromatic protons under all biphasic reaction conditions. The main points to extract from the data presented in Figure 2.2 are the following: 1) the reaction is inhibited

when the concentration of surfactant is low, and 2) broad signals appear in some of the spectra. Table 2.3 and Appendix A.2 shows the quantitative analysis of PTH, pNP, DETP, and MEPTH species in each reaction system after 2100 h reaction time. Retardation of primary reaction products' (pNP and DETP) appearance in the reaction at low CTAC concentrations is consistent with the affinity of the CTAC hydrocarbon chain for the organic interface, thus preventing contact between PTH and the deuteroxide nucleophile.[35]

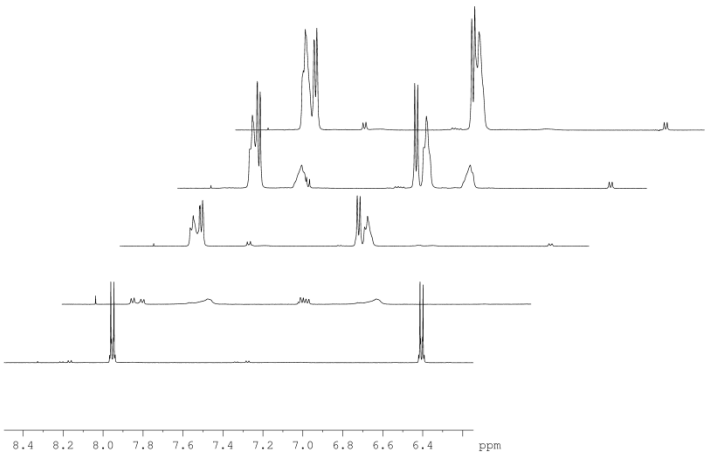

Figure 2.4. ^{1}H NMR spectra for the aromatic region of each reaction system from bottom to top: hydrolyzing control, 0.33 mM CTAC, 3.33 mM CTAC, 10 mM CTAC, 18 mM CTAC, 33.33 mM CTAC.

The broad peaks in Figure 2.2 that appear from 6.9 to 7.1 ppm and from 7.7 to 7.9 ppm can be attributed to bulk PTH that is outside the receiver coil detection region. These lines had 90-degree flip times many times longer than the others in the spectrum. And

their shape suggests they are in a region of poor field homogeneity. Both properties are consistent with signal from the proton-rich PTH below the coil.

Investigations into Stoichiometry Discrepancy

Partition coefficient determination. Analysis of the partition coefficients ($P_{o/w}$) for pNP demonstrated that the affinity of pNP for the aqueous phase changes with surfactant concentration (Figure 2.3). The absence of a phosphorus resonance at 54.9 ppm in the ^{31}P NMR spectrum of the oil layer corresponding to DETP was evidence that DETP was present solely in the aqueous layer, resulting in a negligible partition coefficient for DETP. In the control reaction system without CTAC, pNP had a $P_{o/w}$ of 0.43; pNP favors the aqueous phase over the oil phase. In the 33.3 mM CTAC reaction system, pNP had a $P_{o/w}$ of 4.13; pNP strongly favors the oil phase over the aqueous phase. In all CTAC systems, increasing amounts of CTAC increases the preference of pNP for the PTH phase. The determination of pNP partition coefficients therefore accounts for some of the discrepancy between the pNP and DETP aqueous phase concentrations. Table 2.4 shows a comparison of the control reaction system to the 33.33 mM CTAC reaction system. This shows the discrepancy cannot be fully accounted for by the differences in solubility between the two layers alone. There remains a five to six fold difference in the total amount of primary products formed. The fully tabulated comparisons of pNP and DETP can be found in Appendix A.2.

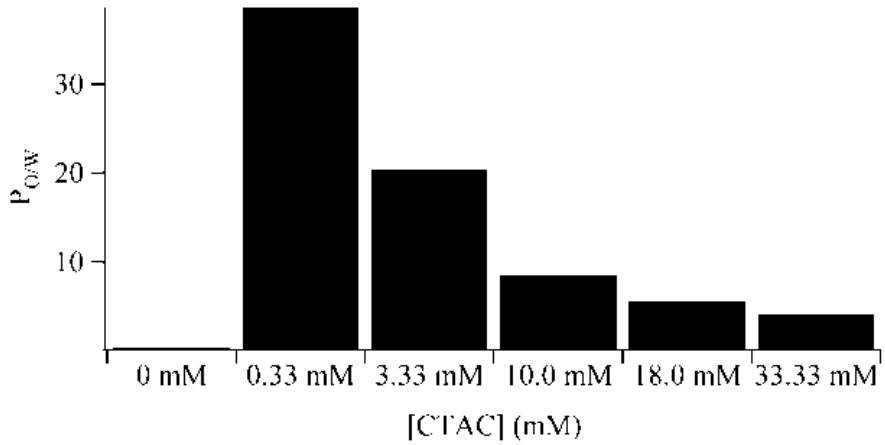

Figure 2.5. Values of $P_{o/w}$ for pNP in each reaction system. Addition of CTAC leads to an increase in the affinity for the oil phase by pNP as compared to the control.

Table 2.4. Comparison of the control system versus the 33.3 mM CTAC system; based on observation of components present in the aqueous phase.

Reaction Conditions	[PTH] (mM)	[pNP] (mM)	[DETP] (mM)	[MEPTH] (mM)	$P_{o/w}$ for pNP	Total pNP (mM)	Total DETP (mM)
Control	0.05	3.56	26.27	0.10	0.43	5.09	26.3
33.3 mM CTAC	23.65	1.00	27.10	7.95	4.13	5.31	27.1

Monitoring of pNP in a mimic control biphasic reaction. We observed a 5 to 6 fold difference in DETP versus pNP concentrations despite the expectation that hydrolysis of PTH should yield a 1:1 ratio of pNP to DETP. To determine whether this difference was due to pNP affixed to the surface of the PTH layer, with DETP dissolved in the aqueous layer, a mimic control biphasic reaction was constructed and monitored by ^{1}H NMR spectroscopy. Based on the assumption that the DETP concentration remains

fixed at its 9.37 mM starting value, and using line D2 as a reference, there was no observable change in the ratio of pNP to DETP for the first 15 h, but it did decline afterwards. The amount of pNP was observed to drop by 1.13 mM relative to DETP in the first week and 1.58 mM after two weeks. Whether any pNP had accumulated at the interface was impossible to determine directly by NMR.[35] To test whether the pNP collected at the PTH interface, the aqueous layer was flushed across the surface of the PTH layer using a Pasteur pipette to bring any interfacial pNP into the aqueous phase. However, the amount of pNP was observed to decrease by 0.27 mM immediately after flushing. After a total of 31 days, with the flushing at day 14, pNP decreased a total of 2.43 mM (0.00018 mmols) relative to DETP. With an initial value of 12.25 mM pNP (0.00582 mmols), this leaves 0.00564 mmols, or 11.9 mM, in the aqueous phase. With these values the $P_{o/w}$ was determined to be 0.20. This is lower than the partition coefficient of 0.43 determined previously, but it might increase over time. This study indicates pNP surface activity is negligible, and the decrease is solely associated with the partition coefficient stated previously.

UV degradation of pNP. To test whether upon exposure to UV light pNP formed free radicals that degrade into products undetectable by NMR spectroscopy, we exposed a mimic sample of the aqueous phase of the reaction control system in the absence of PTH to UV light from the sun for four weeks. The result was that levels of pNP changed by no more than 0.02% based on ^1H signal integration.

Additional reactions of pNP. Another option to account for the observed discrepancy, is pNP reacts with the aqueous phase to form byproducts, eventually CO_2 and H_2O, which are unobservable by NMR.[33] To test this possibility, several samples

were prepared with varying concentrations of NaOD, ranging from 5.33 to 100 mM. These experiments were not biphasic; the reactions were performed with only dissolved PTH. Another simplification was the absence of surfactant in the system. These conditions allowed for the observation of PTH exponential signal decay concurrent with the exponential rise in product signals (pNP and DETP). This exposed an anomaly that becomes clear when the graphs of [PTH], [pNP], and [DETP] are plotted versus time (Figure 2.4).

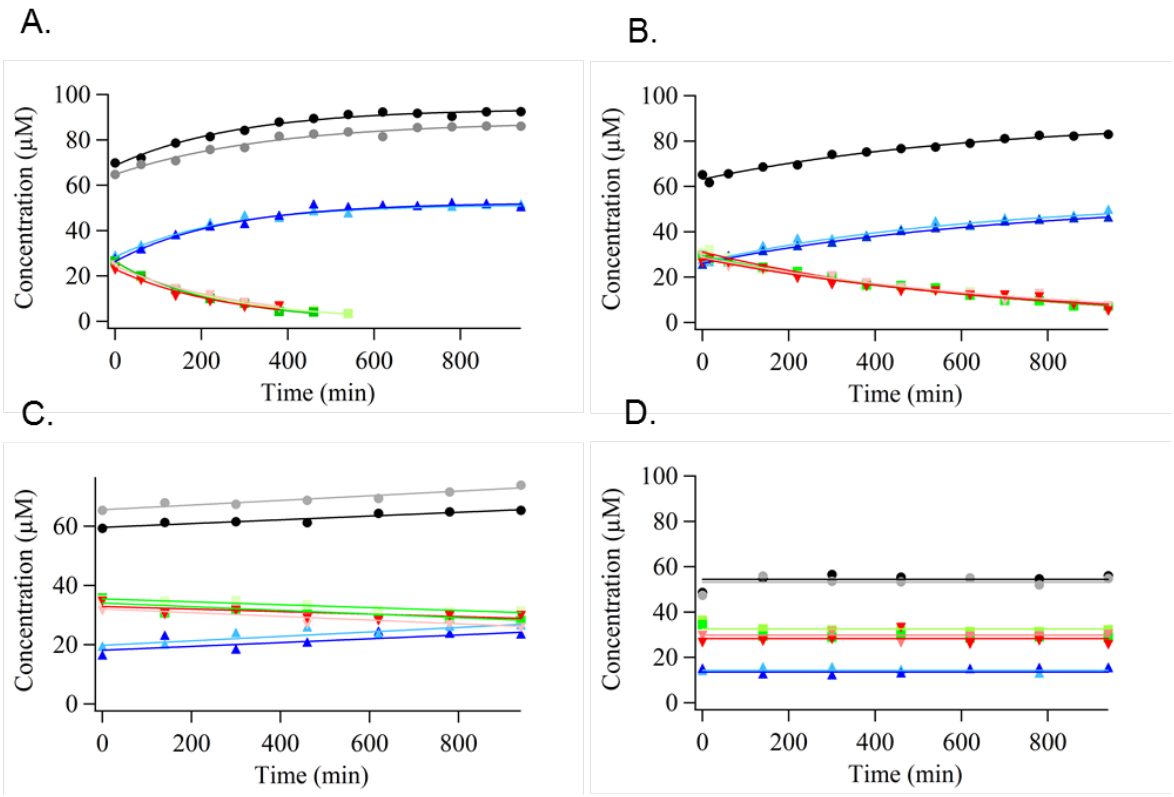

Figure 2.6. Plots of PTH, pNP, and DETP concentrations in A. 100 mM NaOD, B. 33.3 mM NaOD, C. 5.3 mM NaOD, and D. 0 mM NaOD systems. (▼A1 , ▼A2, ■ A3, ■ A4, ▲C1, ▲C2, ● D1 ● D2)

What becomes clear, especially in Figure 2.4 D, is that the pNP is not degrading, i.e. there is no decrease in pNP signal over time. This experiment also revealed that

DETP and pNP were present in the system despite absence of reaction and that DETP concentrations were appreciably higher than pNP concentrations.

This was an unexpected result since the purity of the PTH had been tested by NMR spectroscopy by placing 20 μL of PTH in $CDCl_3$; no DETP or pNP impurities were observed (Figure 2.5). After reviewing the results presented in Figure 2.4, 20 μL of PTH was placed in D6 benzene for analysis, Figure 2.6. D6 Benzene places the dissolved analytes in a different electronic environment than when the same analytes are dissolved in chloroform-d. The pNP and DETP impurities became apparent in the D6 benzene solution and the "neat" PTH solution was calculated to contain 4.4% DETP and 0.2% pNP (Figure 2.6).

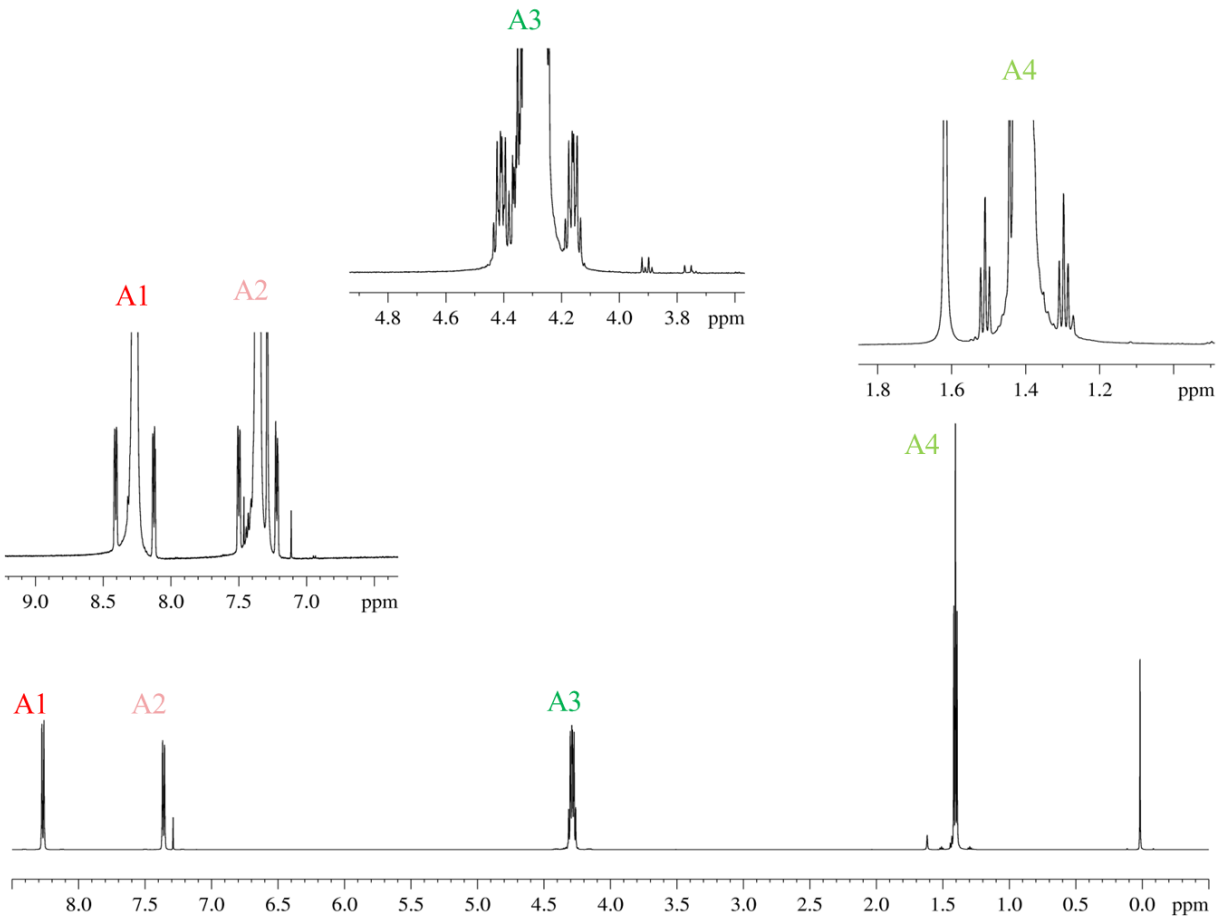

Figure 2.7. ^{1}**H NMR spectrum of PTH in** $CDCl_3$

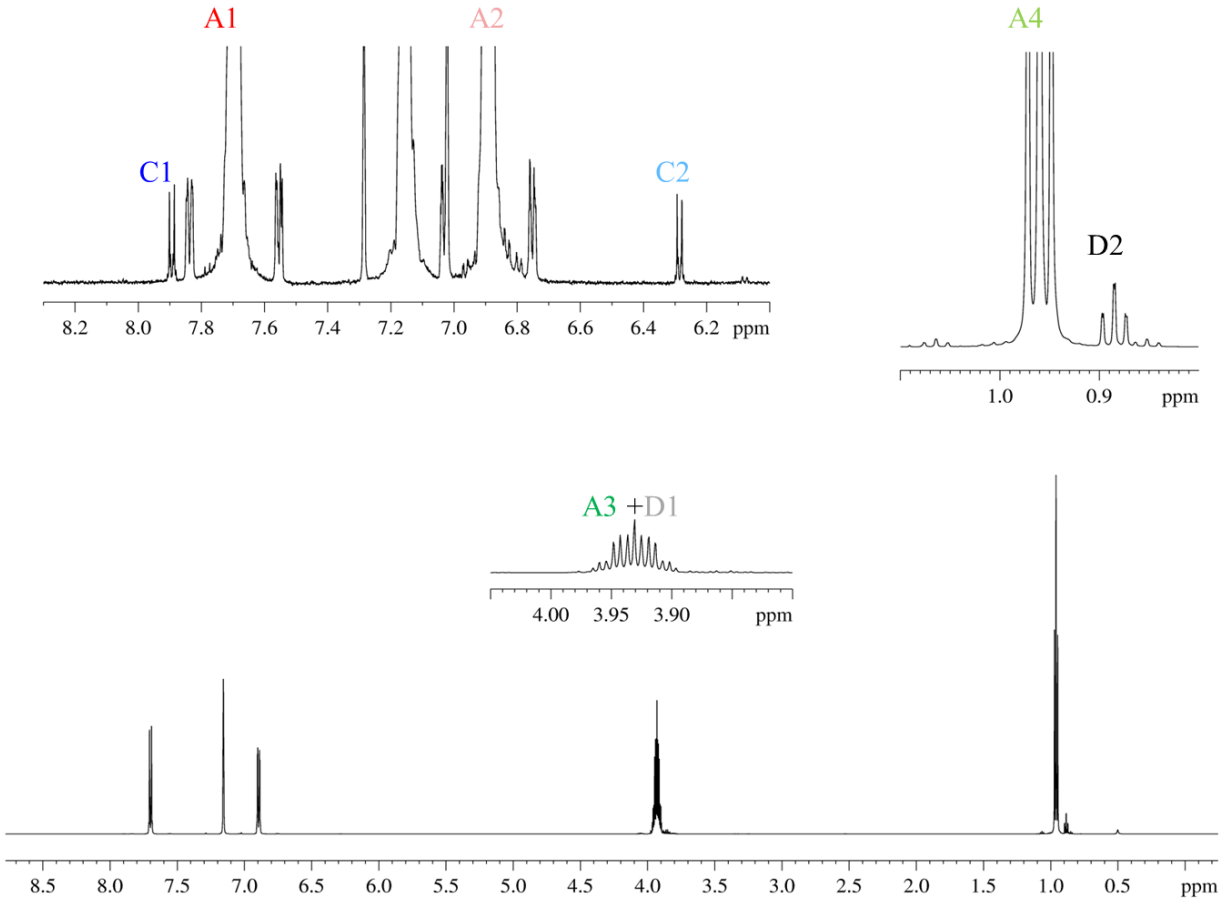

Figure 2.8. ^{1}**H NMR spectrum of PTH in D6 Benzene.**

Conclusions

It can be concluded that transportation of PTH has increased from 0.05 mM and 23.65 mM between the control and the 33.33 mM surfactant experiment. To fully characterize the undisturbed biphasic system, the reaction components were quantified, the partition coefficients for pNP were determined, the surface activity of pNP was evaluated, and the hypothesis of UV degradation of pNP was rejected. Higher concentrations of surfactant lead to increased amounts of MEPTH, indicating the appearance of a reaction mechanism favoring the alternative hydrolysis pathway. The presence of a large amount of unreacted PTH in the aqueous layer is consistent with micellar transport. Thus, with increasing amounts of CTAC, the transportation of PTH into the aqueous phase of an undisturbed biphasic reaction increases. However, it does not increase the degradation of this CWA simulant.

A challenge suggested by this study was to identify the discrepancy between pNP and DETP. Partition coefficient determination for pNP demonstrated that the solubility of pNP increases in the oil layers of the control experiment as compared to the experiments with increasing amounts of CTAC. Taking product solubility into account provided the opportunity to quantify the total amount of pNP in both layers of the biphasic system for each set of conditions studied (Table 2.2 and SI 2). Despite correction for pNP solubility preference in PTH, the total amount of pNP was still calculated to be five to six fold lower than DETP, regardless of surfactant presence.

An attempt to verify the affinity of pNP for the PTH surface showed no indication that pNP was affixing to the surface in sufficient amounts to account for the five to six

fold difference compared to DETP. Over the 2100 h of this experiment, the slight decrease in pNP observed could be accounted for solely by the solubility of pNP in PTH.

Exposing pNP to UV light did not account for an appreciable decrease in pNP solution concentrations after one month. A negligible 0.02% change in the pNP signal was observed over this time-frame.

The discrepancy between pNP and DETP concentrations was finally resolved when the PTH was dissolved in D6 benzene and observed by ^{1}H NMR. The presence of DETP and pNP impurities that had previously been disguised by near-exact overlap of the resonance lines of product and reactants in the solvent $CDCl_3$ became resolved in D6 benzene.

The goal of this work was to characterize the surfactant influence on transportation and hydrolysis of the OP CWA simulant, PTH, in an undisturbed minimally disturbed biphasic reaction medium. An increase of 2 orders of magnitude in the transport of PTH was observed with increasing concentrations of CTAC. The total amount of pNP and DETP formed after 2100 h was within 5% between the control experiment and the 33.3 mM CTAC system; this concludes that the presence of CTAC does not significantly change the long-term rate of reaction between PTH and NaOD. A summary of these findings is tabulated in Table 2.2 and Appendix A.2.

DEPENDENCE OF PARATHION REACTION KINETICS ON OD CONCENTRATION AS CHARACTERIZED BY NMR SPECTROSCOPY:

Introduction

The previous study allowed the impurities in the PTH ampules to be quantified. Correction for pNP and DETP impurities in the PTH starting material allowed the amount of PTH, pNP, and DETP generated solely due to hydrolysis to be distinguished from background impurities. This afforded the possibility to measure the OD-dependant rate of PTH hydrolysis by ^{1}H NMR spectroscopy.

Other studies reporting the kinetics of PTH hydrolysis use UV-VIS,[20, 36, 37] GC,[38] GC-MS,[39, 40] or solid state ^{31}P NMR to monitor the reaction.[41] The issue that arises with some of these analyses is that only one reaction product can be monitored, pNP for the UV detection and DETP for ^{31}P NMR. These reports also carried out the experiments at higher temperatures.[36, 37, 39] To our knowledge, this is the first room temperature kinetics study, as measured by ^{1}H NMR. The value of this approach is that we can monitor all species in the reaction medium simultaneously, under ambient environmental conditions.

In the present study, PTH impurities were identified and quantified as described in chapter 2 using ^{1}H NMR. The experiments reported here focus on measuring how the rate of PTH hydrolysis varies with NaOD concentration. The kinetic rate as a function of nucleophile (OD^{-}) concentration was obtained. The parathion was not purified; instead the concentrations of pNP and DETP impurities were extracted using fitting parameter

describing pseudo-first order kinetics. The pseudo-first order rate equations were derived from Equation 3.1, which describes the actual second-order hydrolysis kinetics

$$\frac{d[PTH]}{dt} = k * [PTH] * [OD]$$

Eq. 3.1

where [PTH] is the concentration of PTH in the system, [OD] is the concentration of OD^- present in the system, and k is the second-order rate constant. Since the OD^- is present in a large amount compared to the PTH, [OD] is essentially constant, and the second order rate equation becomes a pseudo-first order rate equation by setting K_{obs}=k[OD]. Integration of Equation 3.1 yields Eq. 3.2, with the integration constant modified to offset the start of the kinetics by a time, Δt, which is the time between the insertion of PTH into solution and the start of the NMR acquisition. Equations 3.3. and 3.4 were obtained from the relation [pNP]=[DETP]=$C_{o,PTH}$-[PTH].

$$[PTH] = C_{0,PTH} * e^{-K_{obs}*(t+\Delta t)}$$

Eq. 3.2

$$[pNP] = C_{0,pNP} + C_{0,PTH} * (1 - e^{-K_{obs}*(t+\Delta t)})$$

Eq. 3.3

$$[DETP] = C_{0,DETP} + C_{0,PTH} * (1 - e^{-K_{obs}*(t+\Delta t)})$$

Eq. 3.4

Here, $C_{0,PTH}$ is the initial concentration of PTH present in the system, and we have inserted constants $C_{0,pNP}$ and $C_{0,DETP}$ to account for impurities. $C_{0,pNP}$ is the initial amount

of pNP in the sample, which is also the impurity level of pNP. Likewise, $C_{0,DETP}$ is the initial amount of DETP in the sample,.

The 5.3 mM data were treated separated since the rate of reaction is significantly slower, resulting in kinetics that appear linear rather than exponential. A taylor series expansion was used on Equations 3.2-3.4 to obtain Equations 3.5-3.7.

$$[PTH] = -K_{obs} * C_{0,PTH} * e^{-K_{obs}\Delta t} * T + C_{0,PTH} * e^{-K_{obs}\Delta t}$$

Eq. 3.5

$$[pNP] = -K_{obs} * C_{0,PTH} * e^{-K_{obs}\Delta t} * T + C_{0,PTH} * (1 - e^{-K_{obs}\Delta t}) + C_{0,pNP}$$

Eq. 3.6

$$[DETP] = -K_{obs} * C_{0,PTH} * e^{-K_{obs}\Delta t} * T + C_{0,PTH} * (1 - e^{-K_{obs}\Delta t}) + C_{0,DETP}$$

Eq. 3.7

Igor Pro 5.05 was used to plot the data and determine the kinetic rate constants as described in Eq. 3.2-3.7. In some instances, there was overlap interfering with the PTH, pNP, or DETP resonances. This is indicated in this paper by ND (not detectable) in place of the measured value. All available kinetic data are reported.

The pseudo-first order rate constants increased from 0 min^{-1} to 0.0038 min^{-1} over the range from 0 - 100 mM NaOD, respectively. The pH was also dropped below 7 by addition of DCl, to verify that the reaction rate continues to be negligible at low pH. The kinetic fits (Eq. 3.2-3.7) were not only used to obtain kinetic rate constants but, through $C_{0,pNP}$ and $C_{0,DETP}$, to monitor pNP and DETP impurity levels for each ampule of PTH.

The results indicate that impurity levels vary by PTH ampule: the DETP impurities ranged from 3.1% to 11.7% and the pNP impurities ranged from undetectable to 5.2%.

The pseudo-first order rate constants were used to determine the second order rate constant by plotting the pseudo-first order rate constant versus [OD]. The slope of the resulting line is the second order rate constant, which was determined to be 3.90×10^{-5} mM^{-1} ($\pm 8 \times 10^{-7}$) min^{-1}.

Methods

The reaction systems were prepared and monitored in accordance with chapter 2 subsection (d). Table 3.1 contains the concentrations of PTH, NaOD, DCl, and NaCl, in each sample. Refer to the Materials section in chapter 2 for a list of the materials' origins.

Table 3.1. Sample component composition for single phase reaction. A 60 μL quantity of PTH was used to saturate the aqueous phase. The aqueous layer volume (salt, deuterium oxide, and deuteroxide when applicable) was 2700 μL.

Reaction Conditions	PTH (μL)	NaOD (mM)	DCl (mM)	NaCl (mM)
Control	60	0	0	200
Hydrolyzing	60	5.3	0	194.7
Hydrolyzing	60	33.3	0	167.7
Hydrolyzing	60	100	0	100
Acidic	60	0	100	100

Results

100 mM NaOD

The 100 mM NaOD data showed exponential decrease of reactant PTH and an exponential rise of products pNP and DETP. PTH was below noise level in the 500 min data in both trials. An example of PTH decrease and pNP increase in the 100 mM spectra is shown in Figure 3.1.

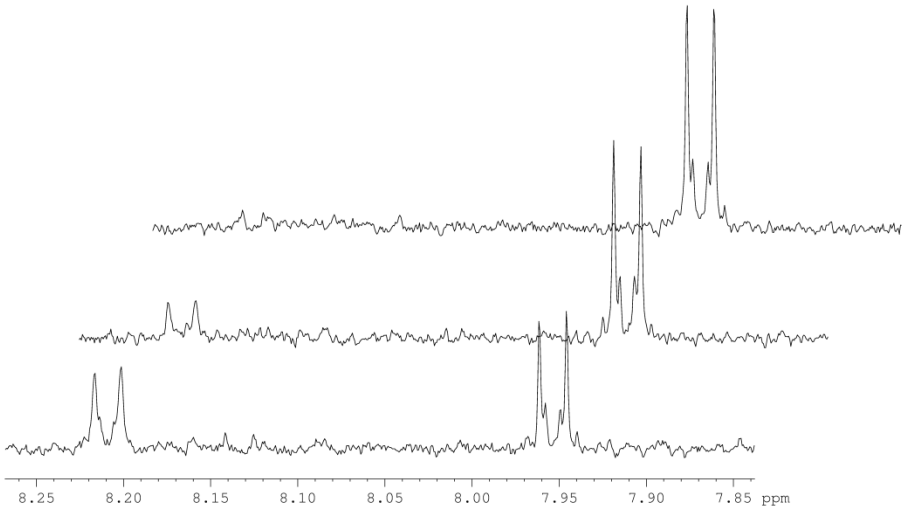

Figure 3.1. ^{1}H NMR of aromatic region of 100 mM NaOD spectra from bottom (0 min) to top (500 min)

In the first trial of the 100 mM NaOD data only three resonances, A1, A2, and A3, of PTH were measured and plotted in Igor Pro 5.05 (Table 2.2). The A4 resonance was compromised by an overlapping resonance. Both DETP signals (D1 and D2) could not be evaluated since overlapping resonances compromised the integration of proton signals. In the second trial, all of the resonances could be measured. Figure 3.2 shows a

plot of PTH and pNP in trial 1, and Figure 3.3 shows a plot of PTH, pNP, and DETP in trial 2, where the NaOD concentration is 100 mM. The constants from the rate equations (Eq 3.2-3.7) are presented in Table 3.2.

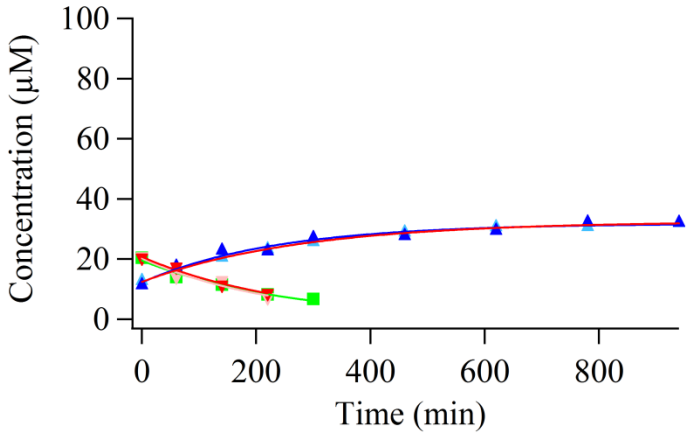

Figure 3.2. Plot of PTH and pNP in trial 1: 100 mM NaOD. (▼A1 , ▼A2, ■ A3, ▲C1, ▲C2)

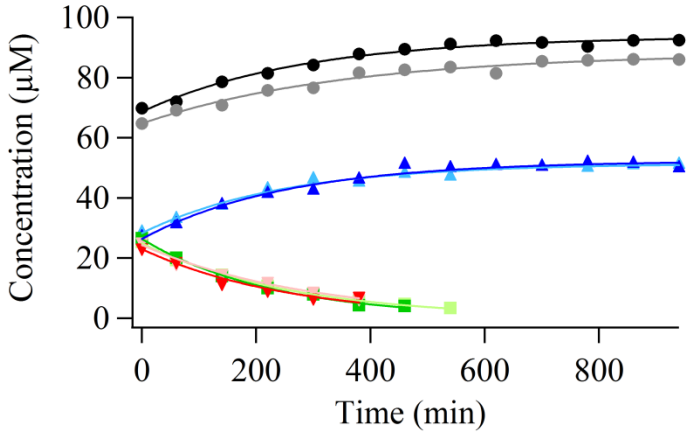

Figure 3.3. Plot of PTH, pNP, and DETP in trial 2: 100 mM NaOD (▼A1 , ▼A2, ■ A3, ■ A4, ▲C1, ▲C2, ● D1, ● D2)

The average rate for both trials is 0.0038 (± 0.0004) min^{-1}. When the initial concentration of PTH was back-calculated using a time constant of 60 min for trial 1 and

41 min for trial 2, the average initial concentration of PTH, including that calculated from the pNP and DETP curves, was found to be 27 (± 2)μM.

Table 3.2. Pseudo-first order rate equation fits for trial 1 and trial 2 for the 100 mM NaOD data. ND indicates that a value was not able to be measured, -- indicates that the value is invalid for that resonance

	Trial 1					**Trial 2**				
Resonance	$C_{0,PTH}$ (μM)	$C_{0,pNP}$ (μM)	$C_{0,DETP}$ (μM)	K_{obs} (min^{-1})	Δt (min)	$C_{0,PTH}$ (μM)	$C_{0,pNP}$ (μM)	$C_{0,DETP}$ (μM)	K_{obs} (min^{-1})	Δt (min)
A1	20.8±0.8	--	--	$4.0 \times 10^{3} \pm 4 \times 10^{-4}$	60	23 ± 1	--	--	$3.9 \times 10^{3} \pm 4 \times 10^{-4}$	41
A2	20 ± 1	--	--	$4.3 \times 10^{3} \pm 9 \times 10^{-4}$	60	24.4±0.9	--	--	$3.4 \times 10^{3} \pm 3 \times 10^{-4}$	41
A3	19.6±0.9	--	--	$3.9 \times 10^{3} \pm 4 \times 10^{-4}$	60	26.4±0.5	--	--	$4.4 \times 10^{3} \pm 2 \times 10^{-4}$	41
A4	ND	--	--	ND	--	25.0±0.3	--	--	$3.8 \times 10^{3} \pm 8 \times 10^{-4}$	41
C1	24 ± 2	8 ± 2	--	$4.3 \times 10^{3} \pm 8 \times 10^{-4}$	60	31 ± 2	22 ± 2	--	$4.0 \times 10^{3} \pm 5 \times 10^{-4}$	41
C2	24.0±0.5	8.6 ± 0.6	--	$3.6 \times 10^{3} \pm 2 \times 10^{-4}$	60	27 ± 1	24 ± 1	--	$4.1 \times 10^{3} \pm 5 \times 10^{-4}$	41
D1	ND	--	ND	ND	--	26 ± 1	--	62 ± 1	$2.8 \times 10^{3} \pm 5 \times 10^{-4}$	41
D2	ND	--	ND	ND	--	29 ± 1	--	65 ± 1	$3.5 \times 10^{3} \pm 4 \times 10^{-4}$	41

33.3 mM NaOD

The 33.3 mM NaOD data also showed exponential decrease of reactant PTH and an exponential rise in products, pNP, and DETP. In trial 1, the PTH concentration was 9.7 μM after the total 980 min reaction time. In trial 2, the PTH concentration reached 7 μM after the entire 980 min reaction time. Figure 3.4 shows NMR spectra of the aromatic proton resonances, between 7.85-8.45 ppm, for the peaks corresponding to PTH and pNP. The PTH peaks are observed to degrade, and the pNP peaks rise as a function of time.

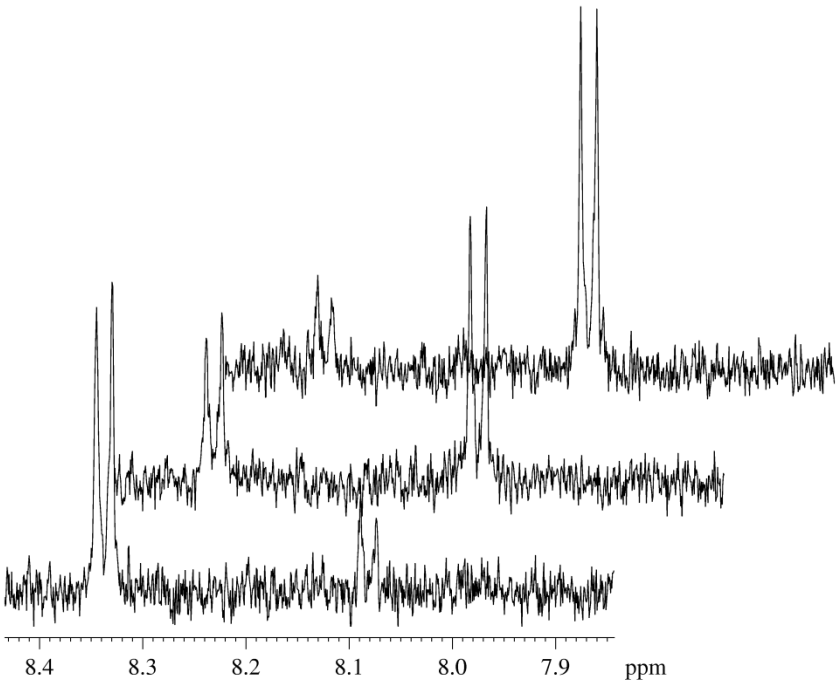

Figure 3.4. ^{1}H NMR of aromatic protons of 33.3 mM NaOD spectra from bottom (0 min) to top (980 min). The PTH (A1) aromatic resonance is downfield, and pNP (C1) aromatic resonance is upfield.

In the both trials of the 33.3 mM NaOD data, all resonances except D1 could be measured and plotted. A plot of trial 1 data is shown in Figure 3.5 and of trial 2 data in figure 3.6, for 33.3 mM data. The constants from the rate equations (Eq 3.2-3.7) are presented in Table 3.2.

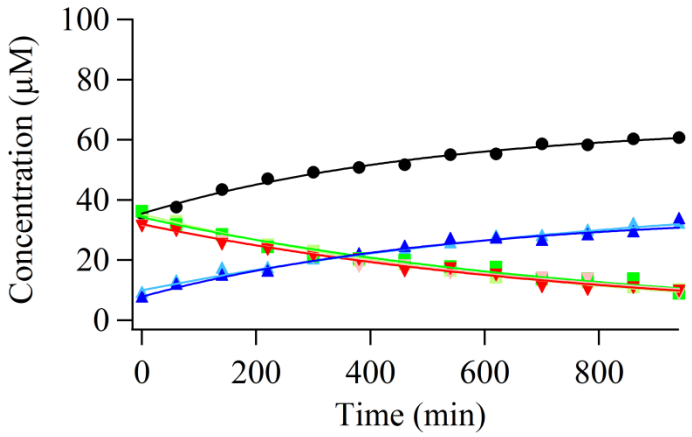

Figure 3.5. Plot of [PTH], [pNP], and [DETP] vs reaction time in trial 1: 33.3 mM NaOD (▼A1 , ▼A2, ■ A3, ■ A4, ▲C1, ▲C2, ●D2)

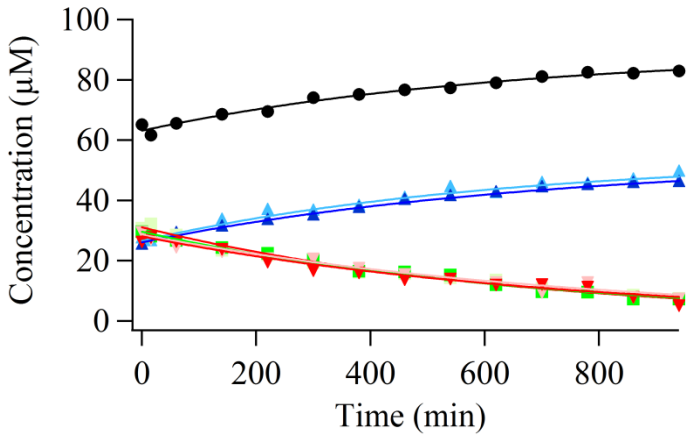

Figure 3.6. Plot of [PTH], [pNP] and [DETP] vs. reaction time in trial 2: 33.3 mM NaOD (▼A1 , ▼A2, ■ A3, ■ A4, ▲C1, ▲C2, ●D2)

The average rate over both trials is 0.0014 (± 0.0002)min^{-1}. When the initial concentration of PTH was back calculated using a time constant of 39 min for trial 1 and

46 min for trial 2, the average initial concentration of PTH, including that which was calculated from the pNP and DETP curves, was found to be 32 (± 3) μM.

Table 3.3. Pseudo-first order rate equation fits for trial 1and trial 2 for the 33.33 mM NaOD data. ND indicates that a value was not able to be measured, -- indicates that the value is invalid for that resonance.

	Trial 1					**Trial 2**				
Resonance	$C_{0,PTH}$ (μM)	$C_{0,pNP}$ (μM)	$C_{0,DETP}$ (μM)	K_{obs} (min^{-1})	Δt (min)	$C_{0,PTH}$ (μM)	$C_{0,pNP}$ (μM)	$C_{0,DETP}$ (μM)	K_{obs} (min^{-1})	Δt (min)
A1	32.0±0.6	--	--	$1.25 \times 10^{3} \pm 6 \times 10^{-5}$	39	28.1±0.7	--	--	$1.34 \times 10^{3} \pm 8 \times 10^{-5}$	41
A2	31.8±0.6	--	--	$1.19 \times 10^{3} \pm 5 \times 10^{-5}$	39	28.7±0.7	--	--	$1.27 \times 10^{3} \pm 7 \times 10^{-5}$	41
A3	34.3±0.9	--	--	$1.24 \times 10^{3} \pm 8 \times 10^{-5}$	39	29.6±0.5	--	--	$1.43 \times 10^{3} \pm 2 \times 10^{-5}$	41
A4	35.3±0.4	--	--	$1.40 \times 10^{3} \pm 8 \times 10^{-5}$	39	31.3±0.5	--	--	$1.52 \times 10^{3} \pm 6 \times 10^{-5}$	41
C1	35 ± 5	8.4 ± 0.8	--	$1.1 \times 10^{3} \pm 3 \times 10^{-4}$	39	30 ± 2	24.3±0.6	--	$1 \times 10^{3} \pm 5 \times 10^{-4}$	41
C2	30 ± 3	6 ± 1	--	$1.9 \times 10^{3} \pm 5 \times 10^{-4}$	39	30 ± 3	25 ± 1	--	$4.1 \times 10^{3} \pm 5 \times 10^{-4}$	41
D1	ND	--	ND	ND	--	ND	--	ND	$2.8 \times 10^{3} \pm 5 \times 10^{-4}$	41
D2	32 ±2	--	33.1±0.9	$1.9 \times 10^{3} \pm 3 \times 10^{-4}$	39	28 ± 3	--	61.2±0.9	$3.5 \times 10^{3} \pm 4 \times 10^{-4}$	41

5.3 mM NaOD

The 5.3 mM NaOD data showed what appeared to be a linear decrease of reactant PTH and a linear rise in products, pNP and DETP. It appears to be linear because the reaction is slow such that at the end of the 16 h observation period there is not enough reaction to exhibit any curvature. In trial 1, the PTH concentration was 26.2 μM after the total 1100 min reaction time. Figure 3.7 shows NMR spectra of the aromatic proton resonances, between 7.85-8.45 ppm, for the peaks corresponding to PTH and pNP. The PTH peaks are observed to degrade, and the pNP peaks rise very slightly as a function of time.

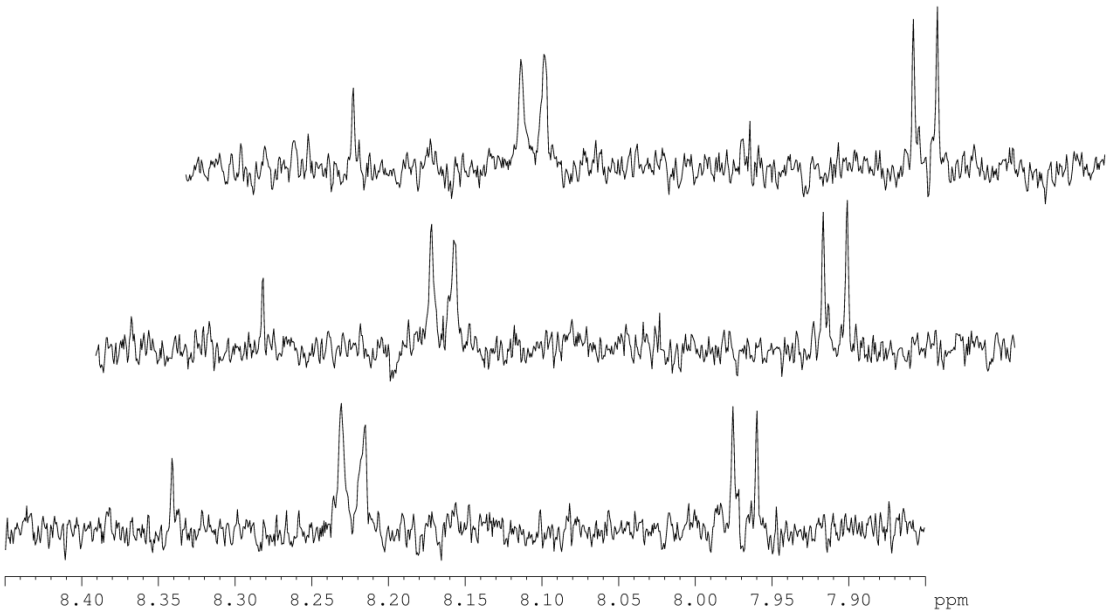

Figure 3.7. ^{1}H NMR of aromatic protons of 5.3 mM NaOD spectra from bottom (0 min) to top (1100 min). PTH (A1) aromatic resonance is downfield, and pNP (C1) aromatic resonance is upfield.

All resonances could be measured. A plot of the concentrations obtained for trial 1 is shown in Figure 3.8, and the constants obtained from the fits are tabulated in Table 3.4. The average rate constant for this trial was found to be 1.9×10^{-4} ($\pm 4 \times 10^{-5}$) min^{-1}.

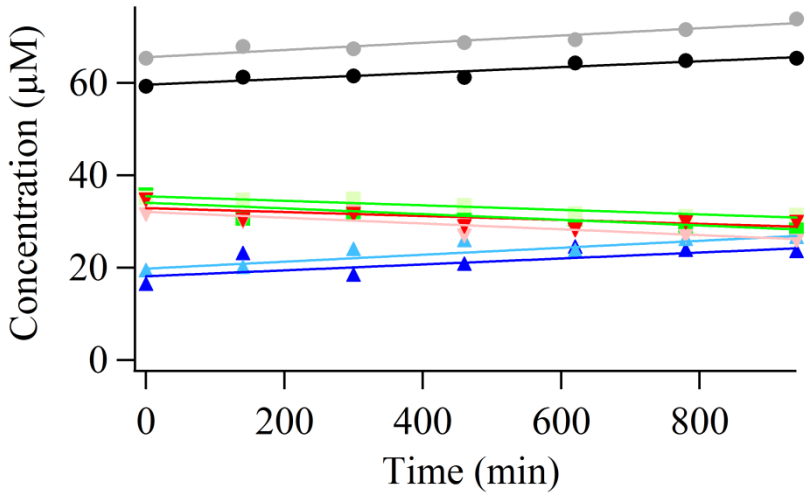

Figure 3.8. Plot of [PTH], [pNP], and [DETP] vs. time in trial 1: 5.3 mM NaOD (▼A1 , ▼A2, ■ A3, ■ A4, ▲C1, ▲C2, ● D1, ● D2)

Table 3.4. Pseudo-first order rate equation fits for trial 1 and trial 2 for the 5.33 mM NaOD data. ND indicates that a value was not able to be measured; -- indicates that the value is invalid for that resonance

	Trial 1				
Resonance	$C_{0,PTH}$ (μM)	$C_{0,pNP}$ (μM)	$C_{0,DETP}$ (μM)	K_{obs} (min^{-1})	Δt (min)
A1	33 ± 1	--	--	$2.0 \times 10^{4} \pm 5 \times 10^{-5}$	156
A2	34 ± 1	--	--	$1.3 \times 10^{4} \pm 6 \times 10^{-5}$	156
A3	35 ± 1	--	--	$1.8 \times 10^{4} \pm 5 \times 10^{-5}$	156
A4	36.2±0.5	--	--	$1.4 \times 10^{4} \pm 2 \times 10^{-5}$	156
C1	--	17 ± 2	--	$2.0 \times 10^{4} \pm 9 \times 10^{-5}$	156
C2	--	19 ± 1	--	$2.3 \times 10^{4} \pm 6 \times 10^{-5}$	156
D1	--	--	58.6±0.7	$1.9 \times 10^{4} \pm 3 \times 10^{-5}$	156
D2	--	--	64.3±0.7	$2.4 \times 10^{4} \pm 3 \times 10^{-5}$	156

0 mM NaOD

The 0 mM NaOD data showed no observable decrease of reactant PTH and no rise of pNP or DETP products. In trial 1, the PTH concentration stayed constant at an average value of 42 μM after the total 980 min reaction time. In trial 2, the PTH concentration also remained constant with an average value of 30μM after the entire 1000 min reaction time. Figure 3.10 shows a stacked plot where the peak intensities of both PTH and pNP stay relatively constant during the entire reaction time.

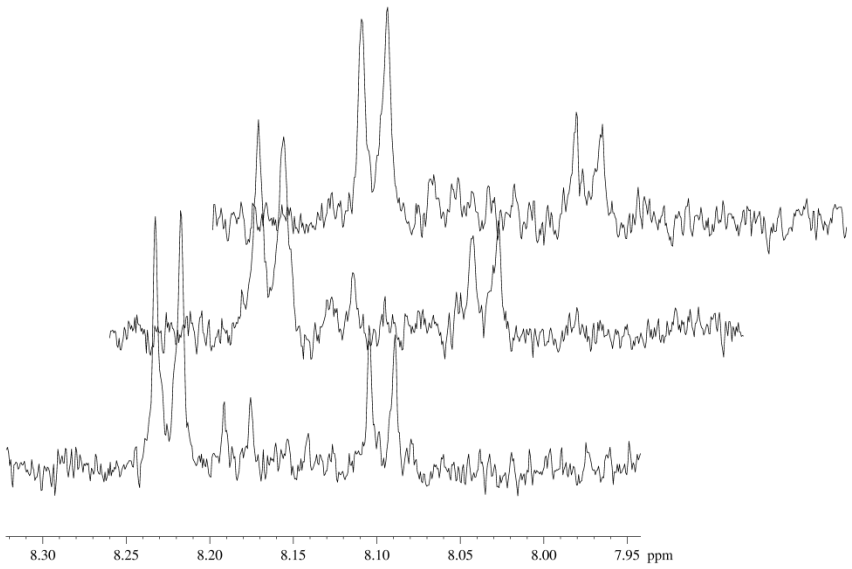

Figure 3.9. ^{1}H NMR of aromatic protons of 0 mM NaOD spectra from bottom (0 min) to top (1000 min). PTH is downfield species, and pNP is upfield species.

Only three PTH resonances were measured for trial 1 of the 0 mM NaOD data since the water peak overlapped with the 4.3 ppm resonance. Both pNP resonances were so small they were undetectable, and only one DETP resonance was measured since there

was an interfering signal with the 3.9 ppm measurement. A plot of the concentrations obtained for trial 1 is shown in Figure 3.10.

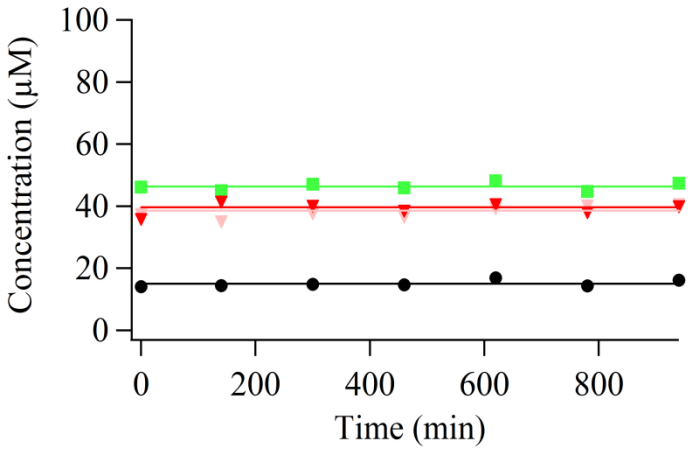

Figure 3.10. Plot of [PTH], [pNP], and [DETP] vs. reaction time in trial 1: 33.3 mM NaOD (▼A1 , ▼A2, ■ A3, ■ A4, ● D2)

In trial 2 all four PTH resonances were monitored. In addition, both aromatic resonances of pNP as well as both aliphatic resonances of DETP were measured and converted into concentrations. The data obtained from trial 2 are shown in Figure 3.11.

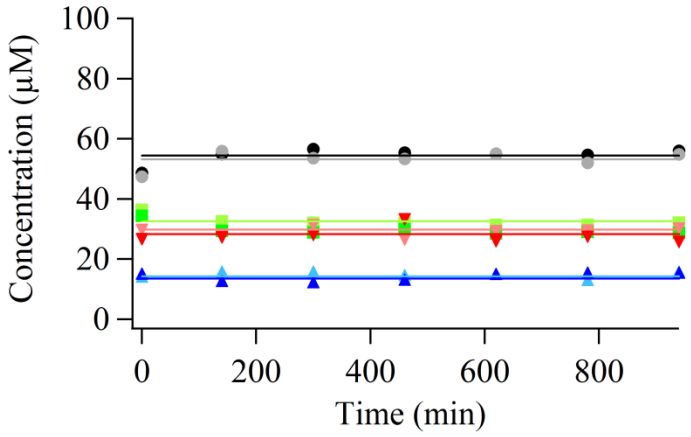

Figure 3.11. Plot of [PTH], [pNP], and [DETP] vs. reaction time in trial 1: 33.3 mM NaOD. (▼A1 , ▼A2, ■A3, ■ A4, ▲C1, ▲C2, ● D1, ● D2)

The average value for PTH over both trials was 35(± 7) μM. The pNP concentration in trial 1 was too small to be detected, while the average DETP concentration in trial 1 was found to be 15.1(± 0.4) μM. In trial 2, the average pNP concentration was 14.0 (± 0.5)μM, and the average DETP concentration was 53.5(± 0.7) μM.

100 mM DCl

The 100 mM DCl data also showed no change of PTH, pNP, or DETP levels. In trial 1, the PTH concentration stayed constant at an average value of 32 μM after the total 985 min reaction time. Figure 3.12 shows NMR spectra with PTH and pNP concentrations unchanged during the entire reaction time.

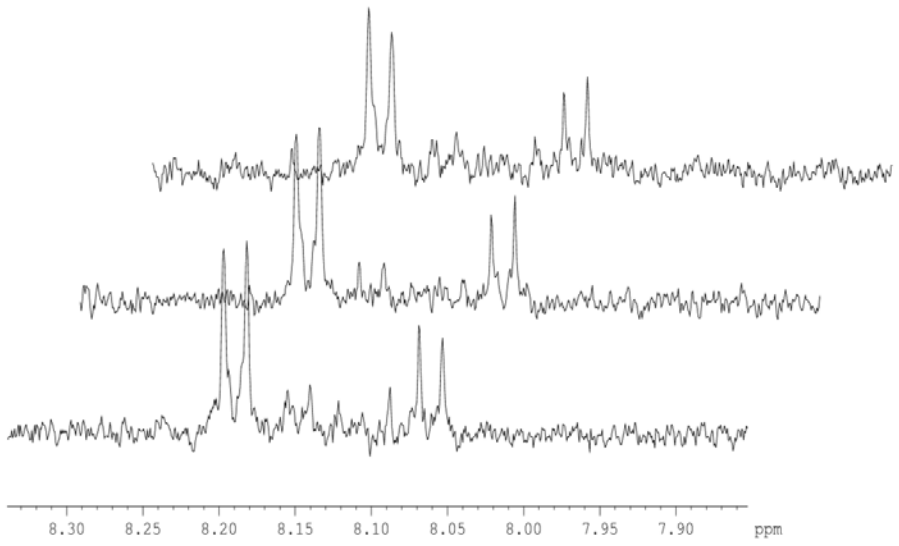

Figure 3.12. ^{1}H NMR of aromatic region of 100 mM DCl spectra from bottom (0 min) to top (985 min). PTH is downfield species, and pNP is upfield species.

Throughout the first trial, all four PTH resonances were monitored, as well as both pNP resonances and the D2 DETP resonances. The calculated concentrations are shown in Figure 3.13.

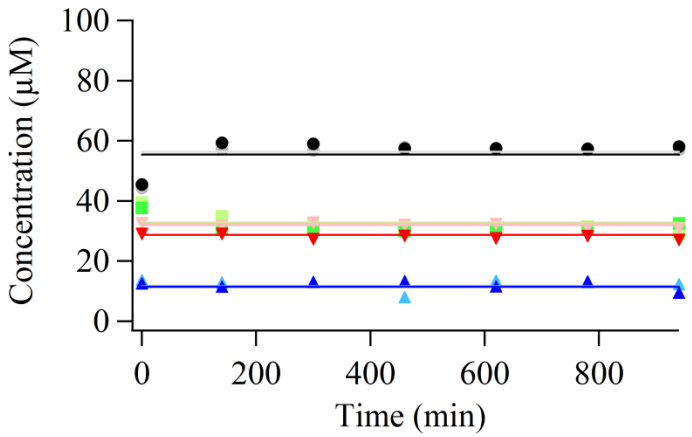

Figure 3.13. Plot of PTH, pNP, and DETP in trial 1: 100 mM DCl. (▼A1 , ▼A2, ■ A3 ppm, ■ A4, ▲C1, ▲C2, ● D2)

The average value of PTH for this trial was 32(± 2) μM. The pNP concentration was averaged to be 11.6 (± 0.1) μM, and the DETP concentration was averaged to be 55.5(± 0.7) μM.

Second Order Rate Constant

The second order rate constant was also determined from these experiments. From a plot of the pseudo-first order rate constant vs. $^{-}$OD concentration, Figure 3.14, the second order rate constant was calculated to be 3.90E-5 (± 9E-7) mM^{-1}* min^{-1}.

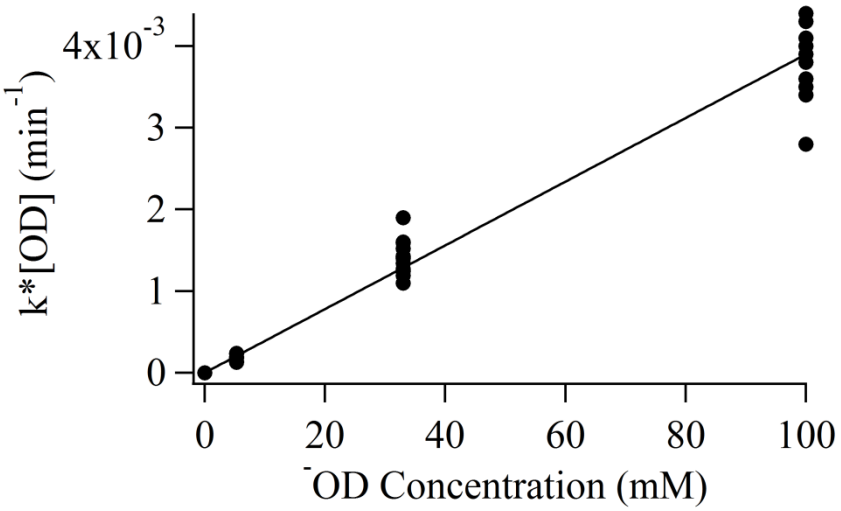

Figure 3.14. Determination of second order rate constant

These results were as expected. The predicted K_{obs} values agreed with the experimental K_{obs} values (Table 3.5). At 50 mM of the NaOD concentration, the rate should be 50% of the 100 mM NaOD rate. This fit predicts that the K_{obs} for the 100 mM is equal to 3.9×10^{-3} min $^{-1}$, while the 50 mM NaOD is equal to 1.95×10^{-3}. This is a factor of two, as expected.

Table 3.5. Comparison of experimental K_{obs} (min^{-1}) to the predicted K_{obs}

[OD] (mM)	$K_{obs,experimental}$ (min^{-1})	$K_{obs,predicted}$ (min^{-1})
100	3.8×10^{-3}	3.9×10^{-3}
33.3	1.4×10^{-3}	1.29×10^{-3}
5.3	1.90×10^{-4}	2.07×10^{-4}
0	0	0

Calculated Impurities

Using the kinetic fits from each of these experiments, the impurity levels for each PTH ampule were determined. Only one experiment was obtained with the first ampule, in which the DETP impurity was calculated to be 3.1% and the pNP impurity was too small to be measured. In the second ampule, the DETP impurity was determined to be 6.2%, and the pNP impurity was 1.6%. The third ampule had a DETP impurity of 11.7% and a pNP impurity of 5.2%. Ampule number four had a DETP impurity of 11.0% and a pNP impurity of 2.6%. Table 3.6 summarizes the impurity levels of DETP and pNP present in each of the four PTH ampules.

Table 3.6. Volume of DETP and pNP impurities separated by ampule based on analysis of a 60 uL PTH aliquot by ^{1}H NMR spectroscopy.

NaOD (mM)	Ampule #1		Ampule #2		Ampule #3		Ampule #4	
	DETP µL	pNP µL	DETP µL	pNP µL	DETP µL	pNP µL	DETP µL	pNP µL
0 mM NaOD-Trial 1	1.8	ND	-	-	-	-	-	-
0 mM NaOD-Trial 2	-	-	-	-	-	-	6.5	1.7
5.3 mM NaOD- Trial 1	-	-	3.4	ND	-	-	-	-
5.3 mM NaOD- Trial 2	-	-	-	-	6.0	3.5	-	-
33.3 mM NaOD- Trial 1	-	-	4.0	0.9	-		-	-
33.33 mM NaOD- Trial 2	-	-	-	-	7.4	3.0	-	-
100 mM NaOD-Trial 1	-	-	ND	1.0	-		-	--
100 mM NaOD-Trial 2	-	-	-	-	7.7	2.8	-	-
100 mM DCl- Trial 1	-	-	-	-	-	-	6.7	1.4
Averages	**1.8**	**ND**	**3.7**	**0.9**	**7.0**	**3.1**	**6.6**	**1.6**

Conclusions

It was determined that the first order rate constant of parathion and NaOD was 3.90E-5 (± 9E-7) mM^{-1}* min^{-1}. To fully characterize the kinetic rates as a function of OD concentration the rate was measured at 100 mM NaOD, 33.33 mM NaOD, 5.3 mM NaOD, 0 mM NaOD, and, in order to verify there was no acid hydrolysis, at 100 mM DCl. Higher concentrations of NaOD lead to increased pseudo first-order rate constant, from 0 min^{-1} to 0.0038 min^{-1}. DETP and pNP impurities were also quantified. The DETP impurities ranged from 3.1% to 11.7%. The pNP impurity levels ranged from not detectable to 5.2% These experiments have presented a method of determining both kinetics and impurity level of a reactant without any purification necessary.

CONCLUSIONS AND SIGNIFICANCE

Our research focused on producing a decontamination method for OP's that could be used both by the military and by the agricultural community. The first study focused on a biphasic system in which the transport of the OP PTH into an aqueous medium was monitored. This study mimicked a real life situation in which a solid would be permeated and saturated by an OP. Once the solid is saturated, there is still a need to extract the OP for complete decontamination. To model these conditions, a liquid-liquid biphasic system was created so that interfacial transport could be observed by NMR spectroscopy, and CTAC was used as a surfactant to enhance PTH transport. This also presented us with the opportunity to report the first study in which all species of the hydrolysis reaction of PTH were monitored by ^{1}H NMR.

The results obtained by this experiment proved to be more difficult to interpret than anticipated. Among the most perplexing result was the stoichiometric discrepancy between reaction products, pNP and DETP. Several experiments were carried out in an attempt to characterize this discrepancy, including: (a) determination of the partition coefficient for pNP between the aqueous and organic phases for each reaction system; (b) pNP surface activity in a control biphasic reaction system; (c) UV degradation study of pNP; and (d) pNP additional reaction study. The answer, although not what we expected, was finally revealed in the final study investigating if pNP was reacting with the aqueous medium to decompose into chemical species not detectable by ^{1}H NMR. While pNP was

not decomposing, plots of the reaction components vs. time revealed what appeared to be an initial impurity of DETP and pNP present within the ampule of pNP. This was unexpected, since the purity of the PTH was tested by dissolving it into CDCl3 and taking a 1H NMR spectrum of the solution; no DETP or pNP was observed. We felt that this warranted further investigation, so an aliquot of PTH was dissolved in deuterated benzene in order to examine the PTH in a different electronic environment. This revealed the DETP and pNP impurity in the PTH ampules.

This result by itself is noteworthy, since we are unaware of any reports where the products of the reaction overlap with the reactant in a ^{1}H NMR spectrum. The reaction between PTH and OD^{-} is a cleavage reaction in which the environment of the product hydrogens is almost identical to the reactant hydrogens. It is conceivable, therefore, that a solvent would exist in which the product and reactant proton resonances would overlap. Whether or not this result of overlapping chemical shift is common would require further investigation.

The CTAC as a transfer agent was successful, resulting in an increase of PTH within the aqueous phase from 0.05 mM to 23.65 mM between the control and the 33.33 mM surfactant experiment. However, the addition of CTAC did not enhance the degradation of PTH as we had anticipated. So, while the addition of CTAC may assist in removing the OP from the saturated solid, it will not enhance the degradation rate.

The CTAC studies provided a foundation for the kinetic studies presented in Chapter 3. The method used for the kinetic studies were drastically different than the method used for the CTAC study; the CTAC studies were done in a minimally disturbed, biphasic heterogeneous system while the kinetic studies were performed in a vortexed,

single phase, homogeneous system. The homogeneous system allowed for the observation of PTH, pNP, and DETP concentrations by 1H NMR. Determination of concentration for reactive species over time resulted in the short term kinetic data. To our knowledge, we have reported the first measurements of kinetics that allows for measurement of all species in the reaction, without quenching the reaction.

From these studies, pseudo-first order rate constants were obtained for NaOD concentrations ranging from 0 mM NaOD (0 min^{-1}) to 100 mM NaOD (3.8 x 10^{-3} min^{-1}). It was determined that the second order rate constant of parathion and NaOD was 3.90E-5 (± 8E-7) mM^{-1}* min^{-1}. This result can be used for the decontamination of OP CWAs since PTH is a known simulant.

Rather than purifying PTH before obtaining kinetic data, we used the kinetic fits to determine the DETP and pNP impurity levels. The DETP impurities ranged from 3.1% to 11.7%. The pNP impurity levels ranged from not detectable to 5.2%. This is significant since this provides a method for obtaining impurity levels of the reactant and obtaining kinetics without any purification necessary.

REFERENCES

1. Tuorinsky, S. D., *Medical Aspects of Chemical Warfare*. United States Dept. of the Army. Office of the Surgeon General. Borden Instititute: Washington, D.C., 1997.

2. Harris, R.; Paxman, J., *A Higher Form of Killing*. Hill and Wang: New York, **1982**; p 74904-74905.

3. Szollosi-Janze, M., *European Review* **2001,** *9*, 97-108.

4. Yang, Y. C.; Baker, J. A.; Ward, J. R., *Chemical Reviews* **1992,** *92* (8), 1729-1743.

5. Beaudet, R. A.; al., e., *Review and Evaluation of Alternative Technologies for Demilitarization of Assembled Chemical Weapons*. National Academy Press: Washington D.C., 1999.

6. Murakami, H.; Birnbaum, A.; Gabriel, P., *Underground: The Tokyo Gas Attack and the Japanese Psyche*. Vintage International: New York, 2001.

7. Skeers, V. M.; Morrissey, B. F., *Journal of Environmental Health* **1995,** *58* (2), 18-23.

8. Ethyl Parathion; Product Cancellation Order. *Register, F.*, Ed. **2006**; Vol. 71, pp 74904-74905.

9. Reregistration Eligibility Decision for Dichlorvos (DDVP). Programs, U. S. E. P. A. O. o. P., Ed. Washington D.C., 2006.

10. Bartelt-Hunt, S. L.; Knappe, D. R. U.; Barlaz, M. A., *Critical Reviews in Environmental Science and Technology* **2008,** *38* (2), 112-136.

11. Wester, R. M.; Tanojo, H.; Maibach, H. I.; Wester, R. C., *Toxicology and Applied Pharmacology* **2000,** *168* (2), 149-152.

12. Manual of Chemical Methods for Pesticides and Devices. Agency, U. S. E. P., Ed. The Association of Official Analytical Chemists: Beltsville, MD, 1982.

13. Ragnarsdottir, K. V., *Journal of the Geological Society* **2000,** *157*, 859-876.

14. Cox, J. R.; Ramsay, O. B., *Chemical Reviews* **1964,** *64* (4), 317-&.

15. Ghosh, K. K.; Sinha, D.; Satnami, M. L.; Dubey, D. K.; Shrivastava, A.; Palepu, R. M.; Dafonte, P. R., *Journal of Colloid and Interface Science* **2006,** *301* (2), 564-568.

16. Ghosh, K. K.; Sinha, D.; Satnami, M. L.; Dubey, D. K.; Rodriguez-Dafonte, P.; Mundhara, G. L., *Langmuir* **2005,** *21* (19), 8664-8669.

17. Balakrishnan, V. K.; Han, X. M.; Vanloon, G. W.; Dust, J. M.; Toullec, J.; Buncel, E., *Langmuir* **2004,** *20* (16), 6586-6593.

18. Zakharova, L. Y.; Mirgorodskaya, A. B.; Zhil'tsova, E. P.; Kudryavtseva, L. A.; Konovalov, A. I., *Russian Chemical Bulletin* **2004,** *53* (7), 1385-1401.

19. Zakharova, L. Y.; Valeeva, F. G.; Kudryavtseva, L. A.; Konovalov, A. I.; Zakharchenko, N. L.; Zuev, Y. F.; Fedotov, V. D., *Russian Chemical Bulletin* **1999,** *48* (12), 2240-2244.

20. Moss, R. A.; Kanamathareddy, S.; Vijayaraghavan, S., *Langmuir* **2001,** *17* (20), 6108-6112.

21. Rav-Acha, C.; Groisman, L.; Mingelgrin, U.; Kirson, Z.; Sasson, Y.; Gerstl, Z., *Environmental Science & Technology* **2007,** *41* (1), 106-111.

22. Myers, D., *Surfactant Science and Technology*. VCH: New York, NY, 1988.

23. Cui, X. H.; Mao, S. Z.; Liu, M. L.; Yuan, H. Z.; Du, Y. R., *Langmuir* **2008,** *24* (19), 10771-10775.

24. Epstein, J.; Kaminski, J. J.; Bodor, N.; Enever, R.; Sowa, J.; Higuchi, T., *Journal of Organic Chemistry* **1978,** *43* (14), 2816-2821.

25. Panuwet, P.; Prapamontol, T.; Chantara, S.; Thavornyuthikarn, P.; Bravo, R.; Restrepo, P.; Walker, R. D.; Williams, B. L.; Needham, L. L.; Barr, D. B., *Archives of Environmental Contamination and Toxicology* **2009,** *57* (3), 623-629.

26. Kotronarou, A.; Mills, G.; Hoffmann, M. R., *Environmental Science & Technology* **1992,** *26* (7), 1460-1462.

27. Zeinali, M.; Torrents, A., *Environmental Science & Technology* **1998,** *32* (15), 2338-2342.

28. Hunter, C. A.; Lawson, K. R.; Perkins, J.; Urch, C. J., *Journal of the Chemical Society-Perkin Transactions 2* **2001,** (5), 651-669.

29. Hunter, C. A.; Meah, M. N.; Sanders, J. K. M., *Journal of the American Chemical Society* **1990,** *112* (15), 5773-5780.

30. Waters, M. L., *Current Opinion in Chemical Biology* **2002,** *6* (6), 736-741.

31. Rahman, M. H.; Chen, H. L.; Chen, S. A.; Chu, P. P. J., *Journal of the Chinese Chemical Society* **2010,** *57* (3B), 490-495.

32. Zhao, S. F.; Ma, H. J.; Wang, M.; Cao, C. Q.; Xiong, J.; Xu, Y. S.; Yao, S. D., *Journal of Hazardous Materials* **2010,** *180* (1-3), 86-90.

33. Bo, L. L.; Quan, X.; Chen, S.; Zhao, H. M.; Zhao, Y. Z., *Water Research* **2006,** *40* (16), 3061-3068.

34. Lide, D. R., *CRC Handbook of Chemistry and Physics*. CRC Press: Boca Raton, FL, 1994.

35. Atkin, R.; Craig, V. S. J.; Wanless, E. J.; Biggs, S., *Journal of Colloid and Interface Science* **2003,** *266* (2), 236-244.

36. Weber, K., *Water Research* **1976,** *10* (3), 237-241.

37. Ketelaar, J. A. A., *Recueil Des Travaux Chimiques Des Pays-Bas-Journal of the Royal Netherlands Chemical Society* **1950,** *69* (4), 649-658.

38. Cowart, R. P.; Bonner, F. L.; Epps, E. A., *Bulletin of Environmental Contamination and Toxicology* **1971,** *6* (3), 231-&.

39. Andreozzi, R.; Ialongo, G.; Marotta, R.; Sanchirico, R., *Journal of Loss Prevention in the Process Industries* **1999,** *12* (4), 315-319.

40. Gomaa, H. M.; Faust, S. D., *Advances in Chemistry Series* **1972,** (111), 189-&.

41. Seger, M. R.; Maciel, G. E., *Environmental Science & Technology* **2006,** *40* (3), 797-802.

.

APPENDIX

Supporting Information for Chapter 2

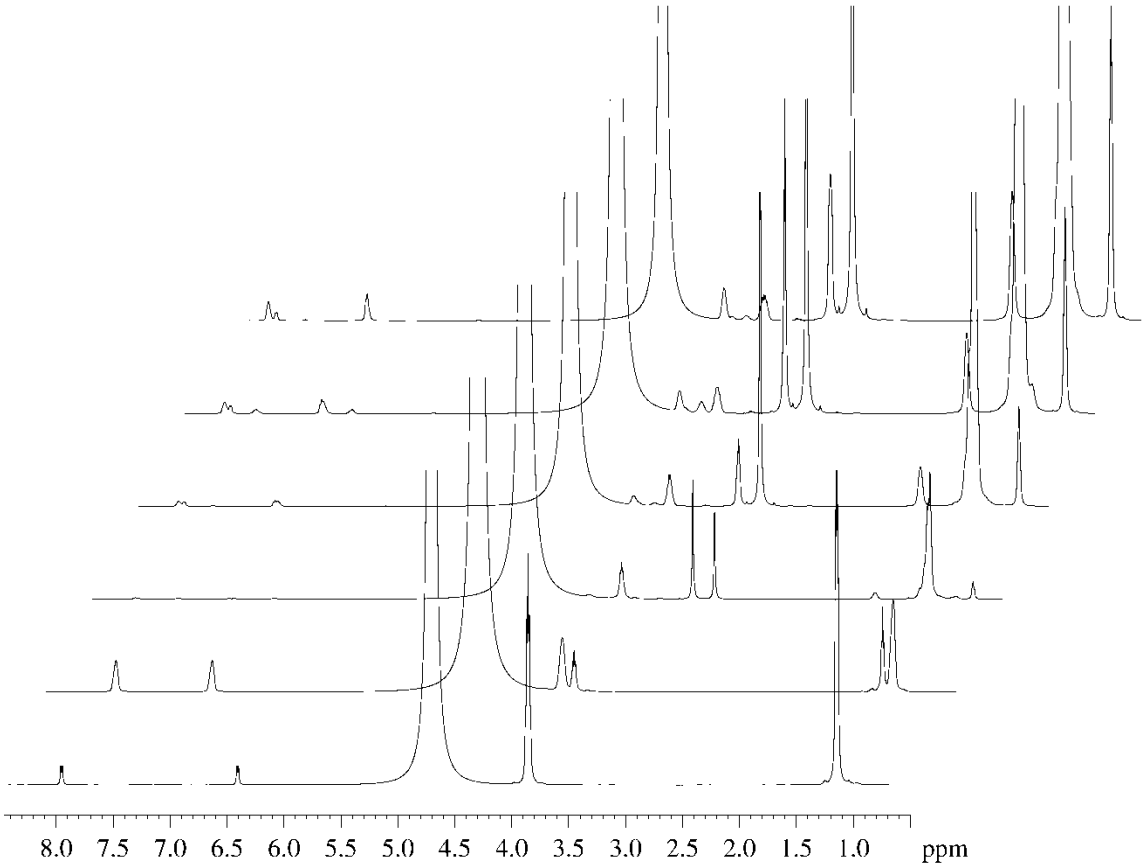

Appendix A.1. ^{1}H NMR spectra ofaqueous phases of biphasic surfactant systems after reaction for 2100 h. All samples contained 33 mM NaOD and NaCl was added to maintain an ionic strength of 100 mM. Surfactant CTAC concentrations from bottom to top: Hydrolyzing control (33.3 mM NaOD and 33.3 mM NaCl), 3.33 mM CTAC, 10 mM CTAC, 18 mM CTAC, 33.3 mM CTAC.

Appendix A.2. Comparison of the biphasic reaction systems based on observation of components present in the aqueous phase of the reaction system. There is a distinct non-stoichiometric relationship between the primary products, pNP and DETP.

Reaction Conditions	[PTH] (mM)	[pNP] (mM)	[DETP] (mM)	[MEPTH] (mM)	Aqueous pH	$P_{o/w}$ for pNP	Total pNP (mM)	Total DETP (mM)
Control	0.05	3.56	26.27	0.10	11.81	0.43	5.10	26.27
0.33 mM CTAC	0.15	0.04	16.81	0.13	9.38	38.61	1.52	16.81
3.33 mM CTAC	1.13	0.14	20.14	0.84	8.66	20.38	3.08	20.14
10.0 mM CTAC	3.78	0.41	21.66	2.75	8.12	8.50	3.90	21.66
18.0 mM CTAC	11.09	0.91	22.61	7.68	8.22	5.59	5.97	22.61
33.3 mM CTAC	23.65	1.00	27.10	7.95	7.64	4.13	5.12	27.10

…